Journal of Andrology, Vol. 22, No. 6, November/December 2001

Structure and Control of a Cell-Cell Adhesion Complex Associated With Spermiation in Rat Seminiferous Epithelium

ROBERT E. CHAPIN,* ROBERT N. WINE,* MARTHA W. HARRIS,* CRISTOPH H. BORCHERS,† AND JOSEPH K. HASEMAN‡

*From the *Reproductive Toxicology Group, †Laboratory of Structural Biology, and ‡Biostatistics Branch, National Toxicology Program, National Institute of Environmental Health Sciences, Research Triangle Park, North Carolina.*

ABSTRACT: Spermiation, the release of late spermatids from the Sertoli cell, is disrupted by a number of toxicants. Control of the spermiation process, and the proteins that interact to adhere mature spermatids to Sertoli cells, is poorly understood. In these studies we used immunohistochemistry, coimmunoprecipitation/Western blotting, and mass spectrometry to refine an earlier model of sperm adhesion proposed by our laboratory. We have identified specific proteins linked together as part of a multiprotein complex, as well as several additional proteins (cortactin, ERK1/2, and 14-3-3 ζ) that may be functioning in both structural and signal transduction roles. The current and prior data suggest that protein phosphorylation is central to the control of spermiation. We also present and characterize an in vitro tubule culture system that allowed functional testing of the spermiation model by pharmacologic manipulation, and yielded data consistent with the importance of protein phosphorylation in spermiation.

Key words: Cadherins, cell adhesions, control, integrins, spermiation.
J Androl 2001;22:1030–1052

Spermiation is the release of mature spermatids from their attachment to Sertoli cells. If spermiation is thought of as the controlled degradation of cell-cell adhesions, a series of testable hypotheses can be explored. A recent review by Vogl et al (2000) shows that such adhesions exist between Sertoli cells and late spermatids, and could mediate the timed and controlled release of these spermatids.

Previous studies by other authors have reported β_1 integrin, actin, vinculin, and a cadherin (Vogl et al, 1985; Grove and Vogl, 1989; Palombi et al, 1992; Byers et al, 1993) at the adluminal edge of the epithelium, where they may be involved in spermatid-Sertoli adhesions. Our previous examination of proteins at the Sertoli–late spermatid junction (Wine and Chapin, 1999) found *N*-cadherin along with proteins known in other systems to be associated intracellularly with controlled junctions (β-catenin, paxillin, $pp60^{src}$, $pp120^{ctn}$ [an Src substrate], Csk [which phosphorylates Src], and vinculin). Indeed, Johnson et al (1999), using a degenerate polymerase chain reaction cloning strategy, reported finding at least 24 cadherins and protocadherins in rat testis and hypothesize the involvement of cadherins in the junction between a Sertoli cell and an elongated spermatid. Because many of these proteins are kinases or substrates for kinases, we hypothesized that the junctions between Sertoli cells and late spermatids are controlled (at least in part) by phosphorylation events inside the Sertoli cell. This hypothesis is merely an extension of a vast literature in other cell types showing that adhesions are controlled by kinases and phosphatases (eg, Collares-Buzato et al, 1998; Kim and Wong, 1998; Inagaki et al, 2000; reviewed in Gumbiner, 2000).

This paper reports the results of efforts to address the following questions: 1) Are the proteins proposed in our hypothetical model (Wine and Chapin, 1999) physically linked with one another as part of a multiprotein complex?, 2) What other proteins may be present and involved in the structure and control of the complex?, and 3) Can the process of spermiation be experimentally perturbed in a way that would provide insight into mechanism?

The actual structure of the previously proposed model (Wine and Chapin, 1999) could be tested by coimmunoprecipitation studies. In this approach, an antibody to a protein of interest (vinculin, for example) is incubated with stage-specific testis lysate. Then the antibody, carrying its antigen and any other proteins that may be bound to the antigen, is separated from the rest of the lysate, separated on a polyacrylamide gel, and the proteins identified by Western blotting or mass spectrometry. Using similar methods, other authors have reported that β_1 integrin coimmunoprecipitates with paxillin (Chen et al, 2000), paxillin coimmunoprecipitates with cortactin (Bowden et al, 1999), and that talin can be coimmuno-

Correspondence to: Robert E. Chapin, DuPont Pharmaceuticals Company, PO Box 30, 1090 Elkton Road, Newark, DE 19714-0030 (e-mail: robert.e.chapin@dupontpharma.com).

Received for publication February 27, 2001; accepted for publication June 12, 2001.

precipitated with FAK_{125} (Chen et al, 1995). Most reports are limited to determining 1 or 2 proteins in addition to the antibody's antigen.

The studies reported here go somewhat further to explore the other proteins that may be involved. The α integrins (Schaller et al, 1993; Fröjdman and Pelliniemi, 1994; Kamata et al, 1995; Trübner et al, 1997) and integrin-linked kinase (ILK; Hannigan et al, 1996; Novak et al, 1998) are logical, given the presence of β_1 integrin. Indeed, ILK has recently been demonstrated to be localized adluminally, and associated with β integrin (Mulholland et al, 2001). Based on the significant amount of actin present adluminally (Vogl and Soucy, 1985; Oko et al, 1991), one would expect proteins that control actin dynamics, such as cortactin (Wu et al, 1991; Wu and Parsons, 1993; Maruyama et al, 1996; Kim and Wong, 1998) and CDC42 (Vojtek and Cooper, 1995). Ras and Rho proteins, and the kinases that control Ras family activities, are also plausible, based on their involvement in other adhesion/signaling systems (for a review, see Braga et al, 1997; Braga, 1999; Kjøller and Hall, 1999; Kuroda et al, 1999; Yamamoto et al, 1999).

Finally, a model is useless if it cannot be tested functionally. An in vitro model of spermiation would be quite useful in the study of this process because it would allow specific pharmacologic manipulations, as well as providing a platform from which to explore the normal and hormonal control of sperm release. For example, because many of the proteins found at the luminal edge are kinases, it is plausible to hypothesize that compounds that interfere with phosphorylation would perturb spermiation. In other cell types, it is known that increased protein phosphorylation leads to cell-cell separation, whereas inhibition of kinase activity can maintain cell-cell adhesions (reviewed in Jockusch et al, 1995). We hypothesized that the same will be true in the seminiferous epithelium. In this paper, we present and characterize an in vitro model for studying spermiation in the rat, and present data consistent with the importance of protein phosphorylation in spermiation.

Materials and Methods

Immunohistochemistry

These visualizations all used the methods described in detail in Wine and Chapin (1999). Each antibody was used at a final working concentration of 5 μg/mL in phosphate buffered saline (PBS). Sections of normal, adult Sprague-Dawley testes, preserved in 1 of the following 6 ways, were used for each antibody: 1) fixed-frozen (FF; in 4% paraformaldehyde for 24 hours then cryosectioned), 2) snap-frozen and fixed in Histochoice (SFHC; Amresco, Solon, Ohio), 3) in 4% paraformaldehyde then paraffin-embedded (P), 4) fixed in 4% paraformaldehyde, paraffin-embedded, then autoclaved (P-AR; for antigen retrieval, 25 pounds for 15 minutes), 5) Bouin-fixed then paraffin-embedded (B), or 6) Bouin-fixed, paraffin-embedded, then autoclaved (B-AR). The antibodies used in these studies are presented in the Table. The biotinylated secondary antibodies were from PharMingen (San Diego, Calif), and were used at a dilution of 1:400 in PBS. All incubations were performed at room temperature. The antibody complex was visualized using aminoethyl carbazole (AEC; Zymed Laboratories, Carlton, Calif), which produces a red reaction product. Sections were counterstained with modified Harris hematoxylin (Sigma Chemical Company, St Louis, Mo).

Tubule Segment Isolation for Coimmunoprecipitation and Culture

Isolation enzymes consisted of 0.25% trypsin (Life Technologies, Rockville, Md) and 0.1% Type 3 collagenase (Worthington Biochemicals, Freehold, NJ) in 20 mL Ca/Mg-free Dulbecco Minimum Essential Medium (DMEM)/F-12, prewarmed to 35°C. Two testes provided ample tissue for either of the two experiments described here. The rat (Sprague-Dawley, Crl:CD, 70–140 days old; Charles River, Raleigh, NC) was killed with an overdose of CO_2. Testes were immediately removed, nearly bisected on the longitudinal axis, and placed into ≈23 mL of prewarmed digestion medium in a 50-mL centrifuge tube, laid horizontally, and shaken vigorously (85 cps, 2.5 inch transit) for 2 minutes at 35°C. After digestion, the enzyme solutions were decanted, and the tissues were combined and washed once with Ca/Mg-free DMEM/F-12, and then washed once with regular DMEM/F-12, decanted to ≈10 mL, and incubated with ≈150 Kunitz units of DNAse at 35°C for 3 minutes with gentle shaking. The tissues were then rinsed three times with DMEM/F-12, and poured into a 100 cm^2 culture dish containing ≈3% fetal bovine serum (FBS; Life Technologies) in DMEM/F-12 for dissection under a stereomicroscope. The FBS prevents the tubules sticking to the plate.

Tubule Segments for Coimmunoprecipitation

To prepare tubule segments for coimmunoprecipitation studies, stage VII-VIII junctions were identified using the criteria of Parvinen et al (1993). Because one of the goals was to assess how these junctional complexes changed during spermiation, 3 segments were isolated: before spermiation (B), during spermiation (D), and after spermiation (A), as indicated by the arrows in Figure 1. To obtain sufficient material to perform coimmunoprecipitations, approximately 120–150 segments of each type were pooled, collected, and placed into separate microfuge tubes for subsequent lysis. The segments during spermiation were necessarily smaller and less frequent, although modulations in the wave of spermatogenesis occasionally allowed for significant lengths of tubules to be collected. These segments contained peritubular cells and all other cellular elements normally found in seminiferous tubules. Prior to lysis, the pooled fragments were pelleted by centrifugation and washed twice with 20 mM phosphate buffer. Following the final wash each pellet was resuspended in 20 μL phosphate/Triton lysis buffer (20 mM phosphate pH 7.2, 150 mM NaCl, 50 mM NaF, 0.5 M Na_3VO_4, and 2% Triton X-100, Complete Mini Protease Inhibitor, EDTA-free (Roche Molecular Biochemicals, Indianapolis, Ind), and trans-

Primary antibodies, types, and sources

Antigen	Molecular Weight (kd)	Antibody Type	Source*	Use†
Actin‡	42	Monoclonal	Chemicon	IHC, WB
N-cadherin‡	130/97–98	Monoclonal	Sigma (clone FA-5), Zymed	IHC, WB, Co-IP
β-catenin‡	92	Monoclonal	Transduction Laboratories, Zymed	IHC, WB, Co-IP
Cdc42	22	Monoclonal	Transduction Laboratories	IHC
Cortactin‡	85/80	Monoclonal	Upstate Biotechnology	IHC, WB, Co-IP
Csk	50	Monoclonal	Transduction Laboratories	IHC
ERK1/2‡	44/42	Monoclonal	Upstate Biotechnology	IHC, WB
Phospho-ERK1/2‡	44/42	Polyclonal	Cell Signaling Technology	IHC, WB
ILK‡	75–80	Polyclonal	Upstate Biotechnology	IHC, WB
α4 integrin‡	80–165	Monoclonal	Chemicon, United States Biological, Antigenix America	WB, Co-IP
α6 integrin‡	118	Monoclonal	Upstate Biotechnology	IHC, WB
β1 integrin‡	130/118	Monoclonal	Transduction Laboratories, Chemicon	IHC, WB
MEK1 MEK 1/2	44–45	Monoclonal, polyclonal	Transduction Laboratories, Cell Signaling Technologies	IHC
Paxillin‡	65–70	Monoclonal	Transduction Laboratories, Zymed	IHC, WB
Phosphoserine	…	Monoclonal	Calbiochem, Accurate	IHC, WB
Phosphothreonine	…	Monoclonal	Calbiochem	IHC, WB
pp120^{ctn}‡	120	Monoclonal	Transduction Laboratories	IHC, WB
Rab3	25	Monoclonal	Transduction Laboratories	IHC
Rab5	25	Monoclonal	Transduction Laboratories	IHC
Rab11	24	Monoclonal	Transduction Laboratories	IHC
Rab27	25	Monoclonal	Transduction Laboratories	IHC
Rac1	21	Monoclonal	Transduction Laboratories	IHC
RalA	24	Monoclonal	Transduction Laboratories	IHC
Ran	25	Monoclonal	Transduction Laboratories	IHC
Rap2	21	Monoclonal	Transduction Laboratories	IHC
Ras	21	Monoclonal	Transduction Laboratories	IHC
Src	60	Monoclonal	Upstate Biotechnology	IHC, WB, Co-IP
β-tubulin‡	55	Monoclonal	Sternberger	IHC, WB, Co-IP
Vinculin‡	130	Monoclonal	Upstate Biotechnology, Chemicon	IHC, WB, Co-IP
14-3-3	30	Polyclonal	Upstate Biotechnology, StressGen Biotechnologies	IHC, WB

* Chemicon, Temecula, Calif; Transduction Laboratories, Franklin Lakes, NJ; Upstate Biotechnology, Lake Placid, NY; Cell Signaling Technology, Beverly, Mass; United States Biological, Swampscott, Mass; Antigenix America, Huntington, NY; Calbiochem, San Diego, Calif; Accurate Chemical, Westbury, NY; Sternberger, Baltimore, Md; Stressgen, Victoria, BC, Canada.

† IHC indicates immunohistochemistry; WB, Western blotting; Co-IP, Coimmunoprecipitation.

‡ Antigens were examined and included into the multiprotein complex after verification by Western blotting. The remaining antigens were evaluated by IHC, found to be at the luminal edge, but could not be verified by Western blotting due to the close proximity of their molecular weight to heavy and light chain of the coimmunoprecipitating antisera. These proteins were not included in the model.

ferred to separate glass microhomogenizers. The tubules were thoroughly homogenized on ice, the resulting lysates were transferred to fresh microfuge tubes, and the lysis was allowed to continue on a Nutator rotating platform for 30 minutes at 4°C. The lysates were clarified by centrifugation for 4 minutes at 14 000 × *g* and the resulting supernatants were transferred to fresh microfuge tubes.

Lysates were precleared by incubating the samples with 5 μg mouse preimmune serum, 5 μg rabbit anti-mouse immunoglobulin G (IgG; Sigma), and prewashed recombinant protein (rprotein) G agarose (Life Technologies) for 30 minutes at 4°C on a Nutator. Following the initial preclearing step, the agarose beads were collected by centrifugation and the resulting supernatants were transferred to fresh microfuge tubes for a second incubation with rprotein G agarose. Upon completion of the second preclearing step, the agarose beads were again collected by centrifugation and the supernatants were transferred to fresh microfuge tubes. An aliquot was removed from each lysate for quantitation of protein (BCA; Pierce, Rockford, Ill).

Coimmunoprecipitations were performed in either 20 mM phosphate or, in the case of vinculin, 25 mM HEPES coimmunoprecipitation buffer pH 7.2 (150 mM NaCl, 50 mM NaF, 0.5 M Na_3VO_4, and 1% Triton X-100, Complete Mini Protease Inhibitor-EDTA free (Roche Molecular Biochemicals). Each coimmunoprecipitation sample contained 250 μg of precleared, staged, seminiferous tubule lysate and 5 μg of primary antiserum. Whenever possible, pooled monoclonal antibodies, not totaling more than 5 μg protein, were used in place of a single antiserum. Negative controls contained 5 μg of mouse preimmune serum in place of primary antiserum. Coimmunoprecipitation samples were allowed to incubate overnight at 4°C on a rotating platform. The addition of rabbit anti-mouse IgG antiserum (Sigma) and continued incubation expanded the initial immune complexes that were formed. These complexes were

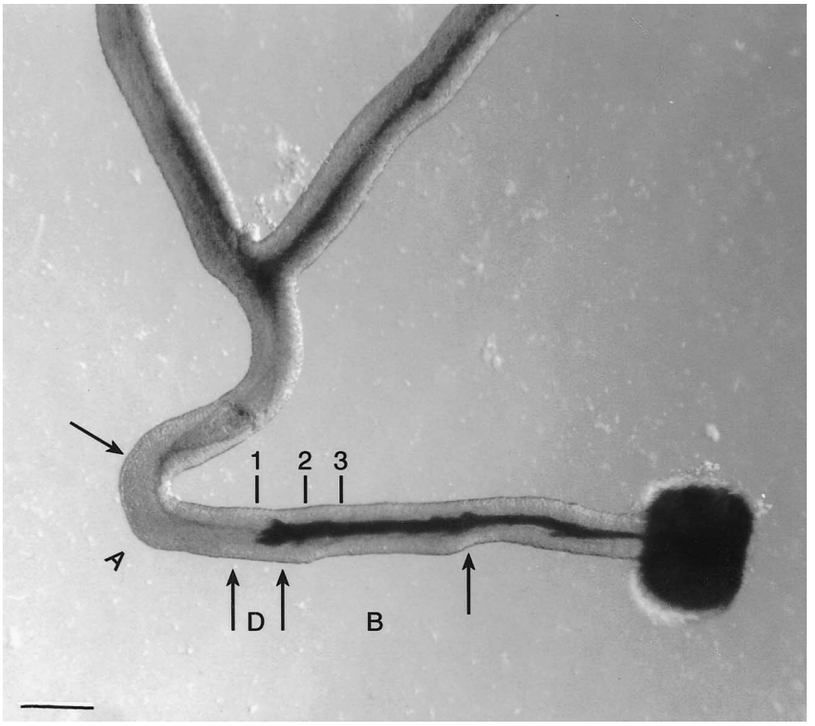

Figure 1. A transilluminated rat seminiferous tubule ≈2 hours after isolation. The arrows beneath the tubule show the length of tubule used to coimmunoprecipitate proteins before (B), during (D), and after (A) spermiation. The numbers above the tubule (1, 2, and 3) indicate the approximate length of tubule that was cut and used for culture. From clearly demarcated tubules such as this one, 2 segments of this length were cut per tubule; several hundred segments were collected, mixed, and divided up among the wells to be cultured. The ''cuff'' on the right shows the massive eversion and epithelial rearrangement that occurs during culture. Finally, the apparent end-to-side anastomosis (Y-joint, or branched tubule) is representative of the several (3–8) such junctions that were found in each animal during culture preparation. Bar = 100 μm.

precipitated with rprotein G agarose and collected by centrifugation. The supernatants were removed and each pellet was washed 3 times with either phosphate or HEPES coimmunoprecipitation buffer followed by 3 additional washes with 20 mM phosphate buffer. Following the final wash the supernatants were aspirated until they just covered the pellets, and 4× NuPage LDS sample buffer (Novex, San Diego, Calif) was added to each sample. The samples were boiled under reducing or nonreducing conditions followed by centrifugation to pellet the free agarose beads. The supernatants were transferred to fresh microfuge tubes and stored on ice until gel electrophoresis and Western blotting.

Western Blotting

Western blots were performed according to routine methods. Briefly, the entire volume of each coimmunoprecipitation reaction was loaded onto 4%–12% NuPage polyacrylamide gels (Novex) and separated according to the method of Laemmli (1970). Resolved proteins were transferred to 0.2-μm nitrocellulose membrane using Towbin transfer buffer followed by blocking in Superblock (Pierce). The antigen or antigens of interest were detected using SuperSignal West Pico chemiluminescent substrate and the images were acquired on a Kodak ImageStation 440CF (Eastman Kodak, Rochester, NY). Biotinylated markers (Bio-Rad, Hercules, Calif) and SeeBlue Plus 2 prestained standards (Novex) were separated in conjunction with the samples to allow for accurate determination of molecular weight and efficiency of transfer, respectively. Ten micrograms of total protein from lysates of whole rat testis, HeLa, human endothelial, and A431 cells were included on each gel as positive controls to verify the specificity of the antisera and confirm the presence of the protein in rat testis. All Western blots were performed at least 3 times. Because of the scope of this project, efficiency was important, so each membrane was often probed with multiple primary antibodies simultaneously if the antigens were of sufficiently different molecular weight.

Protein Identification by Microsequencing

Concomitant to investigating the protein complex by traditional coimmunoprecipitation/Western blotting and immunohistochemistry, experiments were performed attempting to identify unknown proteins found in the coimmunoprecipitation samples. These experiments were performed using either a chemical cross-linker or Western blotting with phosphoserine, threonine, or tyrosine antisera, followed by mass spectrometry.

For specific cross-linking and fluorescent labeling of proteins linked with one another in the multiprotein complexes, we chose sulfosuccinimidyl 2-(7-azido-4-methylcoumarin-3-acetamido) ethyl-1-3′-dithiopropinate (SAED; Pierce). Coimmunoprecipitations using paxillin as the precipitating antiserum were prepared essentially as described above. However, following the final washing of captured immune complexes the samples were la-

beled with SAED as previously described (Borchers and Tomer, 1999). Using this method, only proteins that are physically linked to one another as part of a multiprotein complex receive a fluorescent azido-methylcoumarin tag incorporated into its structure. Labeled proteins were visualized by illumination with a longwave UV light source, and the image was captured on an ImageStation 440 CF (Eastman Kodak). The bands of interest were excised for further treatment as described below.

Protein bands demonstrating an increase or decrease in amino acid–specific phosphorylation by Western blotting during the time of sperm release were identified on companion Coomassie-stained gels by laying the Western film directly over the companion gel. Bands of interest were excised for further treatment as described immediately below.

In-gel digests were performed on the excised protein bands and the samples were prepared for analysis by Matrix-Assisted Laser Desorption/Ionization (MALDI; Perseptive Biosystems, Framingham, Mass) and Quadrapole Time Of Flight (Q-TOF; Micromass, Altrincham, United Kingdom) mass spectroscopy as previously described (Borchers and Tomer, 1999; Borchers et al, 2000). The peptide mass data were searched using the program MS-Fit against a nonredundant database (NCBlnr) located at the University of California San Francisco (http://prospector.ucsf.edu).

Tubule Segments for Culture

Methods for culturing tubule segments largely followed those initially elaborated in Li et al (1997). The exception is that Li strove to keep the ends of the tubule segments closed, whereas no such attempt was made here; it was hoped that the ends of the tubules would evert. Using transillumination, the Stage VIII-IX junction was identified as above, and 2 1.5-mm segments immediately before this junction were cut with iridectomy scissors (Figure 1). These sections from numerous junctions were collected into a group, mixed thoroughly, and partitioned into groups of 13–14 segments, each group aspirated into a wide-bore 200-μL pipette tip, and placed into 2 mL of culture medium in a 12-well Costar plate. Tubule segments were cultured in DMEM/F-12 containing (per 100 mL of medium) 1 mL insulin-transferrin-selenium plus linoleic acid and bovine serum albumin (ITS+), 0.003 μg epidermal growth factor (EGF), and 29 μg dihydrotestosterone and testosterone (DHT/T), and rocked at 16 cycles per minute overnight at 32°C in 95% air/5% CO_2. Chemical treatments of the tubules were formulated immediately prior to culture and placed into each well so that when tubules were placed in culture, their exposure to the treatment condition began. All dimethyl sulfoxide (DMSO) vehicles were used at the lowest possible concentration, between 1 μL DMSO/mL DMEM and 0.1 μL DMSO/mL DMEM. Controls for exposures in DMSO had DMSO at the same concentration as the exposed wells. The following treatments were used:

- Sodium azide (Sigma) 350 μg/2 mL, which ≈4-times a LD_{50} (Merck Index), dissolved in DMEM/F-12.
- Peroxovanadate, a tyrosine phosphatase inhibitor, which should increase the amount of phosphorylated proteins within the tubules, used in dose range of 0.125 μM to 3.75 μM (Ruff et al, 1997) in PBS. In addition to or as a consequence of inhibiting protein tyrosine phosphatases, peroxovanadate also activates mitogen-activated protein (MAP) kinase, a serine-threonine kinase (Zhao et al, 1996).
- Okadaic acid (Calbiochem), an inhibitor of serine/threonine phosphatases, 10–100 nM (Haystead et al, 1989; Gjertsen et al, 1994), dissolved in DMSO.
- Staurosporine (Calbiochem, San Diego, Calif), a broad-spectrum inhibitor of serine-threonine kinases, 0.1–100 nM (Oka et al, 1986), in DMSO. Staurosporine also inhibits protein kinase C (PKC; Couldwell et al, 1994). To try to determine the involvement of PKC in spermiation, other inhibitors of PKC were tried in two experiments. All of these inhibitors were from Calbiochem: bisindolylmaleimide 1 (30, 300 nM); a myristoylated protein kinase C inhibitor 19–27 (10, 100 nM); and RO-32-0432 (60, 600 nM), all dissolved in DMSO.
- Geldanamycin (Calbiochem), an inhibitor of tyrosine kinases, and specifically Src, was used at 0.1–3 μM (Mimnaugh et al, 1996) in DMSO.
- Other tyrosine kinase inhibitors evaluated in more limited experimental designs were herbimycin A (0.1–10 μM), H7 (1–100 μM), H8 (0.1–100 μM), and lavendustin C (0.05–5 μM), all from Calbiochem and all in DMSO.

Sertoli cells are known to respond to EGF (Mallea et al, 1986) and have receptors to follicle stimulating hormone (FSH; reviewed in Means et al, 1978). To explore other possible controls of spermiation, an EGF receptor blocker (PD168393, Calbiochem) was evaluated, as was omission of EGF from the culture medium. Two experiments covaried the amounts of EGF and FSH (Sigma) in the culture: from none, to circulating amounts, to 10× the blood levels. And because neurotransmitters were found to be beneficial for the maintenance of advanced function of seminal vesicle cells in vitro (Kinghorn et al, 1987), acetylcholine, norepinephrine, and serotonin were added to one culture to determine whether they would increase the proportion of released cells.

Bacitracin, a protein disulfide isomerase inhibitor, has been reported to be a selective inhibitor of β_1 integrin-mediated lymphocyte adhesion (Mou et al, 1998). Because of evidence suggesting a role for β_1 integrin in the process of spermiation (Palombi et al, 1992; Salanova et al, 1995), experiments were carried out to evaluate the potential of bacitracin to disrupt adhesion between late spermatids and the seminiferous epithelium. Bacitracin dissolved in DMEM/F-12 was used at a concentration of 0.01–3.0 mM.

In each experiment there were 3–4 wells per treatment, and each experiment was repeated 2–6 times. The tubule segments were cultured overnight (16–20 hours). At the end of the culture period, segments were removed by aspiration in 20–30 μL of medium and placed into 2 mL of DMEM/F-12 and homogenized for 3 seconds with a Tekmar Ultra-Turrax homogenizer (Tekmar-Dohrman, Cincinnati, Ohio). The remaining culture medium was removed to a labeled tube. Sperm released into the culture medium and the unreleased homogenization-resistant spermatid heads were counted using a hemocytometer. The proportion of total sperm in each well that had been released was calculated.

Histology

Tubule segments in 2 wells per dose for selected chemicals were fixed in 3% paraformaldehyde/2% glutaraldehyde for ≈24 hours,

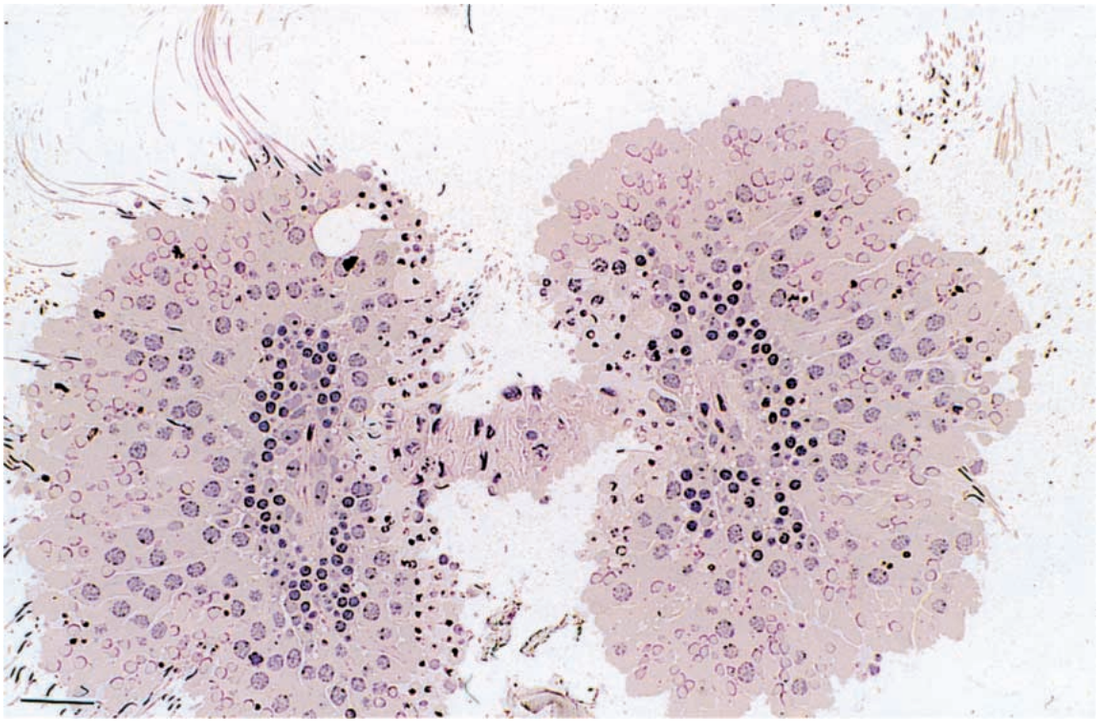

Figure 2. Light-level photomicrograph of control tubule, fixed in glutaraldehyde, and embedded in glycol methacrylate after ≈16 hours in culture. Note the everted epithelium retains its basic organization and orientation, and there is little if any cell death. Bar = 20 μm.

rinsed in PBS, embedded into Immuno-Bed (Polysciences, Warrington, Penn), sectioned, and stained with periodic acid–Schiff-hematoxylin (Figure 2). This was done to determine if increases in sperm release were the result of normal release from the seminiferous epithelium, rather than sperm shed from disintegrating epithelium.

Statistics

Analysis of variance procedures were used to assess the effect of dose effects, experiment-to-experiment variability, and the interaction between these two factors on the proportion of released sperm in the tubule culture experiments. Pairwise comparisons with controls were made by the Dunnett test using the $P < .05$ level of significance. Statistical analyses were carried out both with and without a variance-stabilizing arc sine transformation applied to the proportions. For the data reported here, the arc sine transformation had no significant effect on study results. For data reported in the text, an asterisk (*) indicates significant difference ($P < .05$) from the control value.

Results

Immunohistochemistry

The distribution for each antibody is presented below. In most cases, the staining was present using more than one preparation, but was strongest, or most clear, in the preparation presented. In two cases (β_1 and α_6 integrin) there was no staining in any tissue preparation method other than the one presented. ILK stained only FF or SFHC-fixed sections. With each immunohistochemical reaction performed, a control section in which mouse or rabbit preimmune serum replaced the primary antisera, was included. Figure 3A is representative of the control sections achieved with each reaction. In these control sections, no staining was noted within the seminiferous epithelium. The fixative that worked best for each antibody is abbreviated in parentheses immediately after each antigen. Because the focus of our investigation was the proteins involved in spermiation, the immunohistochemistry results described here are confined to stage VIII tubules.

β_1 Integrin (Para-AR)—The cell adhesion receptor subgroup β_1 integrin (Figure 3B) was localized at sites of intraepithelial contact and was strongest above the spermatocyte level, between the round spermatids and along the luminal edge in stage VIII tubules. This distribution differs with previous reports of β_1 integrin distribution in rat seminiferous epithelia (Palombi et al, 1992; Salanova et al, 1995) in that staining is not confined to the ectoplasmic specialization. Our staining pattern was consistent, and its variance from previous reports may be due to differences in antibody specificity, fixation conditions, antigen retrieval, or a combination of these factors.

α_6 Integrin (FF)—The strongest staining for the α_6 in-

tegrin chain was in interstitial cells and myoid cells surrounding the tubule. In the photo (Figure 3C), staining was present at what appeared to be sites of cell contact between round spermatids, although precise localization is not possible at this magnification. Staining was also present in and around recently shed residual bodies. The distribution of α_6 integrin was reminiscent of the distribution of β_1 integrin in that the staining appeared between cells, and this staining seemed to begin above the pachytene spermatocyte cell layer. As with β_1 integrin, the distribution of α_6 integrin was consistent with previously reported work (Salanova et al, 1995).

α_4 Integrin (FF)—Despite the disappointing structural preservation often obtained with FF tissue sections, a significant amount of staining for rat specific α_4 integrin was seen distributed throughout the various cell types in stage VIII tubules (Figure 3D). The pattern of staining for the α_4 integrin chain was similar to, yet less well defined, than that seen for α_6 integrin, and appeared to be within the cell cytoplasm. An intense reaction product was observed in the peritubular cells.

ILK (FF)—ILK is a serine/threonine kinase known to interact with the cytoplasmic tail of β_1 integrin (Delcommenne et al, 1998), and whose overexpression can result in a loss of cell-cell adhesion (Novak et al, 1998). Staining for ILK (Figure 3E) was clearly present and strong in all cells within the tubule. Although precise localization was not possible at this level of resolution, the photomicrograph allows visualization of punctate foci of staining around the adluminal edge of the epithelium; perhaps a specific structure accumulated within residual bodies or in phagocytic vacuoles. The protein was clearly not concentrated in peritubular cells or vasculature.

Cortactin (B)—Staining for the actin binding protein cortactin was strongest in peritubular cells and around the heads of elongate spermatids in stage VII-VIII tubules (Figure 3F). It was also clearly present around residual bodies and the concave side of the heads of elongate spermatids (inset), consistent with Sertoli cell localization. There was occasional basal staining around pachytene spermatocytes. Both the adluminal staining and the peritubular staining patterns mimic the pattern shown for actin (Vogl et al, 1985).

Ras (P-AR)—Ras proteins relay signals from tyrosine kinases to the nucleus through a network of serine/threonine kinases (Yamamoto et al, 1999). Ras staining in paraformaldehyde sections (Figure 4A) appeared as faint granular foci apparently between germ cells, and around residual bodies. Higher magnification (inset) indicates that staining is not concentrated within residual bodies, but appears lightly between them, which would be consistent with a Sertoli location. In some Bouin sections, Ras protein could occasionally be seen in Sertoli cell columns (not shown).

Ral A (B-AR)—The guanosine 5′-triphosphate (GTP) binding protein RalA was detected faintly in the cytoplasm of intermediate spermatogonia up to early pachytene spermatocytes (Figure 4B). In mid and later pachytenes, staining appears circumferential around these cells (at the light microscope level, it is impossible to distinguish whether staining is inside or outside these germ cells). Round spermatids are not detectably positive. Elongate spermatids have considerable staining between them, which does not appear to be in the long spermatid cytoplasm. Concentrated adluminally (inset), Ral A appears to be around, not in, residual bodies, which would be consistent with a Sertoli cell location.

Rac 1 (B)—The Ras-related GTPase Rac plays a role in actin dynamics (Braga, 2000). Rac1 demonstrated strong basal staining around the circumference of the tubule, consistent with both early germ and Sertoli cell staining (Figure 4C). Occasional columnar staining in tubules suggested a Sertoli cytoplasm localization for Rac1, with adluminal concentration of the protein in stage VIII tubules (inset). There is an immunohistochemical signal in the round spermatid layer, but much fainter than the presumptive Sertoli or adluminal signal intensities. The adluminal signal could be from either germ cells or Sertoli cells, but the pattern for Rac 1 is similar to the cortactin and actin staining, which would be consistent with Sertoli cell localization.

ERK1/2 (B or B-AR)—Not visible in either peritubular

→

Figure 3. **(A)** A representative immunohistochemical control section in which mouse isotype control solution was substituted for primary antiserum. There was no aminoethyl carbazole (AEC) chromagen observed throughout the tissue section, indicating a lack of nonspecific reaction product. Bar = 10 μm. β_1 integrin staining in stage VIII seminiferous epithelium **(B)** appeared predominantly at sites of cell-cell contact (arrows), and along the adluminal edge, where it appeared to envelop residual bodies. This is more clearly seen at higher magnification (inset), where there is an apparent membrane localization of chromagen near the proximal heads of mature spermatids. α_6 integrin staining **(C)** was most intense in peritubular cells in all tubules observed and localized to sites of cell-cell contact between round spermatids (arrows) and around residual bodies at the adluminal edge (arrowheads). Like α_6 integrin, the staining pattern for α_4 integrin **(D)** was extremely heavy in peritubular cells (*) and appeared to localize to intercellular junctions (arrows). Staining was fairly uniform throughout the cells within a tubule, with a slight concentration around residual bodies (arrowheads). ILK staining appeared as punctate foci along the adluminal edge in stage VIII tubules **(E)** (arrows). The protein appears to be distributed throughout the cytoplasm of all the cells in a tubule, but appeared absent from nuclei. Higher magnification (inset) shows a lack of signal within residual bodies. Cortactin staining **(F)** was discretely localized to peritubular cells (arrow). Prominent staining was noted along the adluminal edge, localized around the heads of mature sperm. This is more evident in the inset, where the protein can be seen located along the proximal concave side of mature sperm (arrowhead). Staining did not appear within residual bodies. Bar **(B–F)** = 7.5 μm.

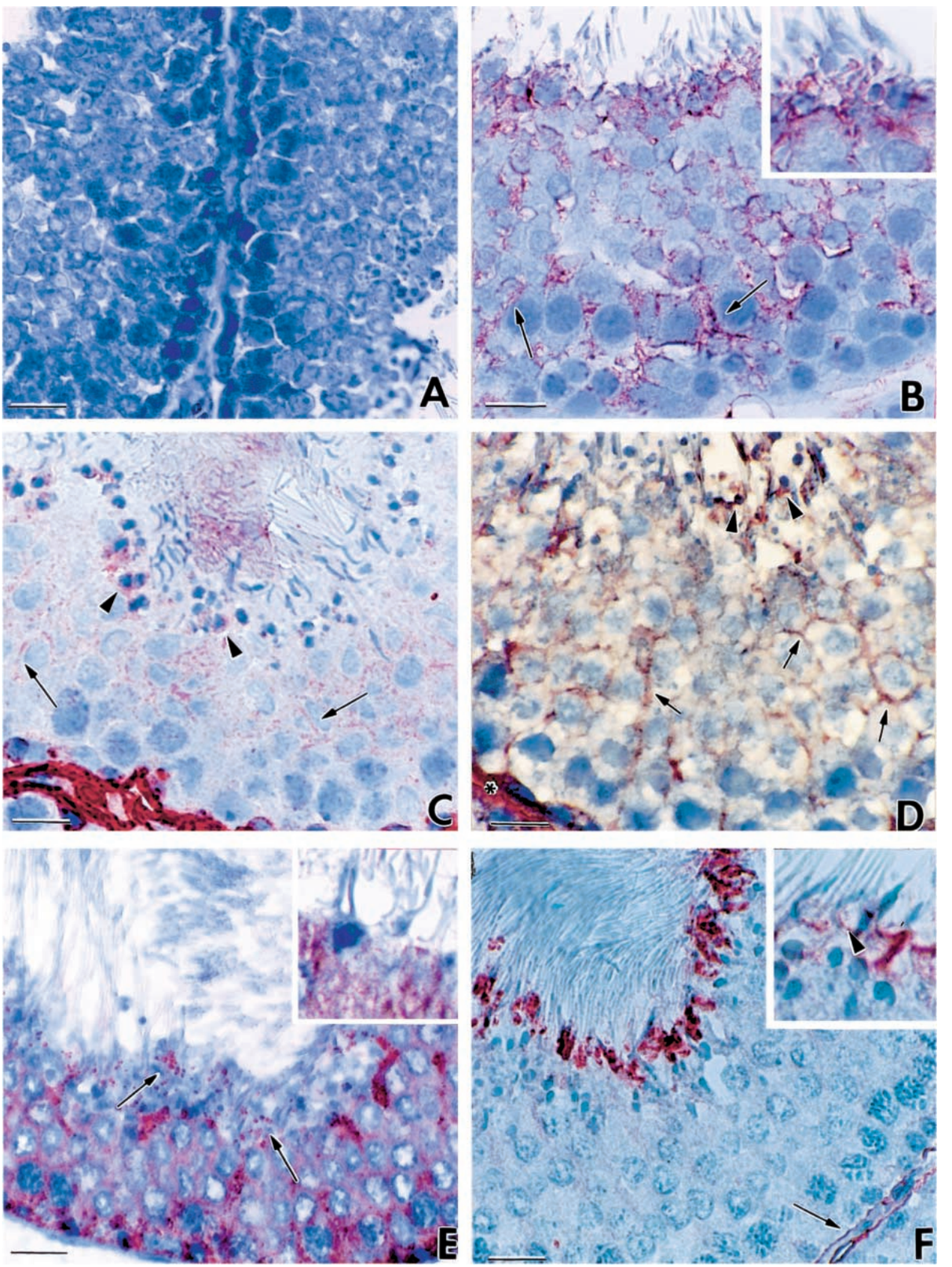
A
B
C
D
E
F

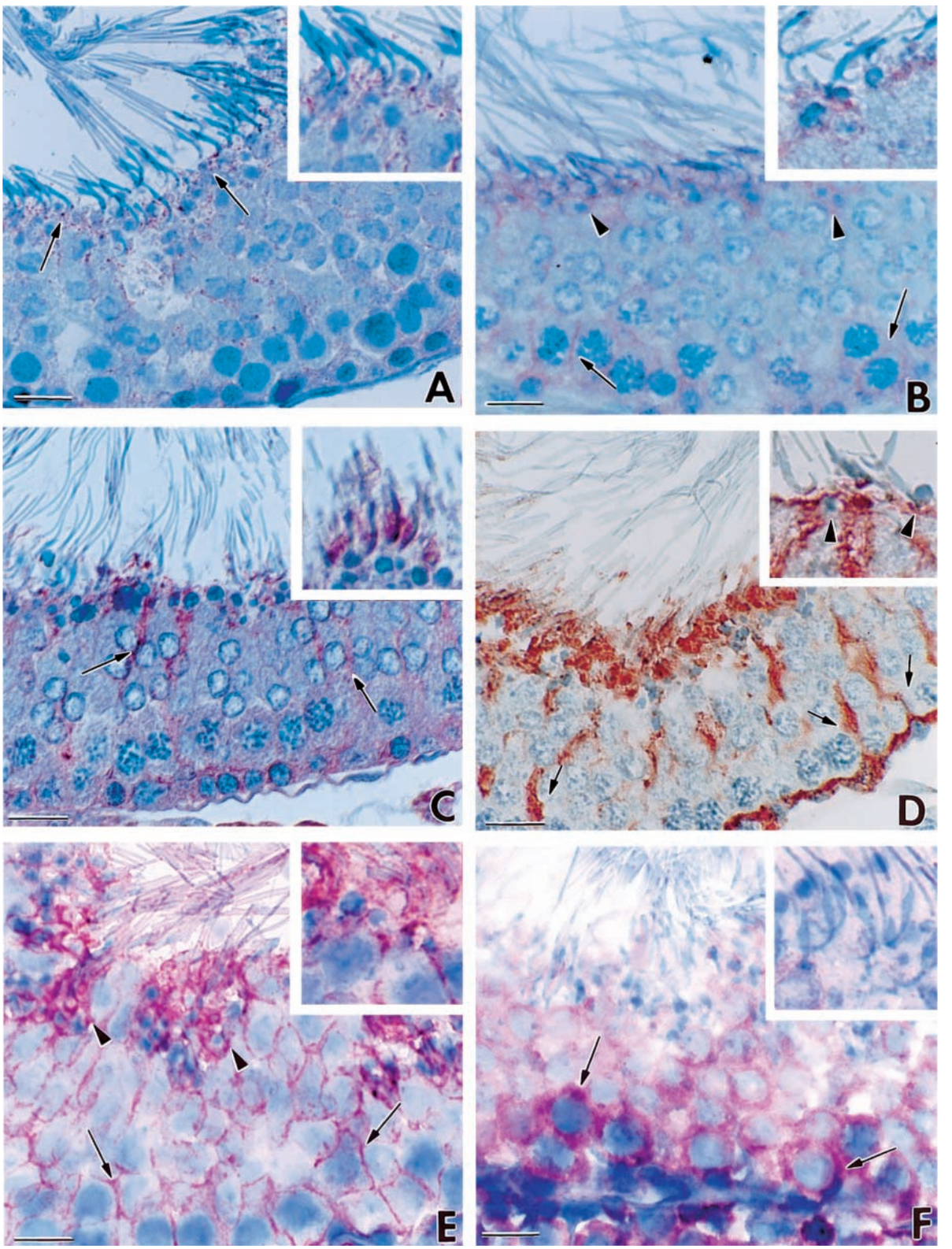
A
B
C
D
E
F

or interstitial cells, staining for the extracellular signal-regulated kinases (ERK) 1 and 2 was quite prominent in the basal portion of stage VIII tubules (Figure 4D). Often extending up in columns from Sertoli cell nuclei, ERK1/2 staining formed a prominent radial staining pattern similar to Sertoli tubulin distribution (Johnson et al, 1991). In stage VIII tubules, intense signal was present around clumps of elongated spermatids and around, but not in, residual bodies. Faint staining was observed between round spermatids both before and after spermiation. In stage IX and X tubules, a prominent signal was present around the basal edge of elongating spermatids, in a pattern reminiscent of actin distribution changes (not shown).

Phospho-ERK1/2 (FF)—The presence of ERK1/2 protein at the luminal edge of the seminiferous epithelium does not necessarily mean that the kinase is in an active state. Antisera against threonine/tyrosine phosphorylated (active) ERK1/2 (Figure 4E) stained areas of cell cytoplasm, at what appear to be sites of cell contact between adjacent cells, throughout the epithelium in stage VIII tubules. At the light microscopic level it cannot be determined whether the staining is between cells or is in the interior cytoplasm along the membrane. Heavy adluminal staining was observed around the heads of elongated spermatids and residual bodies (inset) in a pattern virtually identical to that seen with antiserum against the inactive form of ERK1/2. The intense staining along the adluminal edge of the tubule was observed only in stage VIII tubules and had disappeared by stage X. The involvement of ERK1/2 in the process of sperm release was further investigated by Western blotting (see below).

MEK1/2 (FF)—MEK1/2 are dual specificity kinases that activate ERK1/2 by phosphorylating both threonine and tyrosine residues (see Seger and Krebs, 1995 for review). Antisera against MEK1/2 (Figure 4F) heavily stained early and late spermatocyte cytoplasm, becoming less prominent in the cytoplasm of round spermatids. Staining was weakly visible in cytoplasm of Sertoli, interstitial, and vascular cells, and absent in residual bodies or peritubular cells. Thus, staining for MEK appeared present in most cells within a tubule. There is a striking contrast in apparent distribution between MEK1/2 and ERK1/2, particularly around the elongated spermatids, given their known interrelationships in other cell types, suggesting that the relationship between these two proteins may differ in the testis, compared with other cell types.

CDC42 (B-AR)—CDC42 is guanine nucleotide triphosphate (GTP) binding protein and Rho family member, and is believed to be important in the regulation of cytoskeletal organization (Burridge, 1999). Staining for CDC42 (Figure 5A) was strongest in interstitial cells and basally in tubules. This basal staining appears to be in the cytoplasm of early germ cells and pachytene spermatocytes. There is less stain intensity in round spermatids, and then greater staining intensity in the Sertoli cell cytoplasm enveloping elongating and elongated spermatids (inset). There is also some apparent columnar and peri-round spermatid staining. All of this staining was completely blocked by blocking peptide (not shown).

Phospho-serine (SFHC and B)—Antiserum against phosphorylated serine residues gave a staining pattern that was strongest in the interstitium (Figure 5B). In Bouins-fixed sections, there is significant staining adluminally in stage VIII tubules, which appears to be incorporated in the elongated spermatid cytoplasm (inset), and faintly present in some residual bodies. There was no clear cellular delineation within the epithelium, appearing fairly evenly and faintly in germ cells and Sertoli cells, except for this noticeable concentration adluminally in stage VIII tubules.

Phospho-threonine (B-AR)—Figure 5C demonstrates the staining pattern of proteins containing phosphorylated threonine in a late stage VIII tubule. No staining was visible in peritubular cells and most vasculature cells, and was absent from nuclei of all cell types. Staining was scattered throughout the cytoplasm of all other cell types, particularly pachytene spermatocytes, and appeared occasionally in radial arrays within the epithelium. However, the most prominent localization of phospho-threonine proteins was at the adluminal edge of the epithelium

←

Figure 4. **(A)** The distribution for Ras in stage VIII tubules was strongest along the adluminal edge, appearing as granular foci (arrows). The inset shows the relationship of Ras protein to the heads of elongated spermatids. Signal for Ras was sprinkled as discrete foci throughout most cell types, although precise localization at this magnification was not possible. RalA, in many of the sections observed, localized to sites of intercellular contact **(B)** (arrows). A strong and consistent signal was observed along the adluminal edge of the epithelium, where it was seen surrounding residual bodies (arrowheads). Rac1 staining was prominent around spermatocytes in the basal portion of tubules **(C)**, and in the cytoplasm of pachytene spermatocytes. Columns of staining between round spermatids were occasionally observed (arrows), terminating at the adluminal edge. Higher magnification (inset) shows the protein surrounding the heads of elongated spermatids. ERK1/2 staining **(D)** also appeared as columns extending up from the basement membrane to the adluminal edge in stage VIII tubules, suggesting a Sertoli cell cytoplasmic localization (arrows). Heavy staining around the adluminal edge was associated with the heads of elongated spermatids, but did not appear to be incorporated into residual bodies (arrowheads, inset). Staining for phosphorylated (active) ERK1/2 **(E)** localized to sites of cell-cell contact throughout the epithelium (arrows). Heavy staining was observed around the adluminal edge, surrounding the heads of elongated spermatids and clusters of residual bodies (arrowheads). In contrast, staining for MEK1/2 protein **(F)** was strongest in the cytoplasm of pachytene spermatocytes (arrows). Staining intensity was decreased in the cytoplasm of round spermatids and was faint along the adluminal edges of stage VIII tubules. Bar = 7.5 μm.

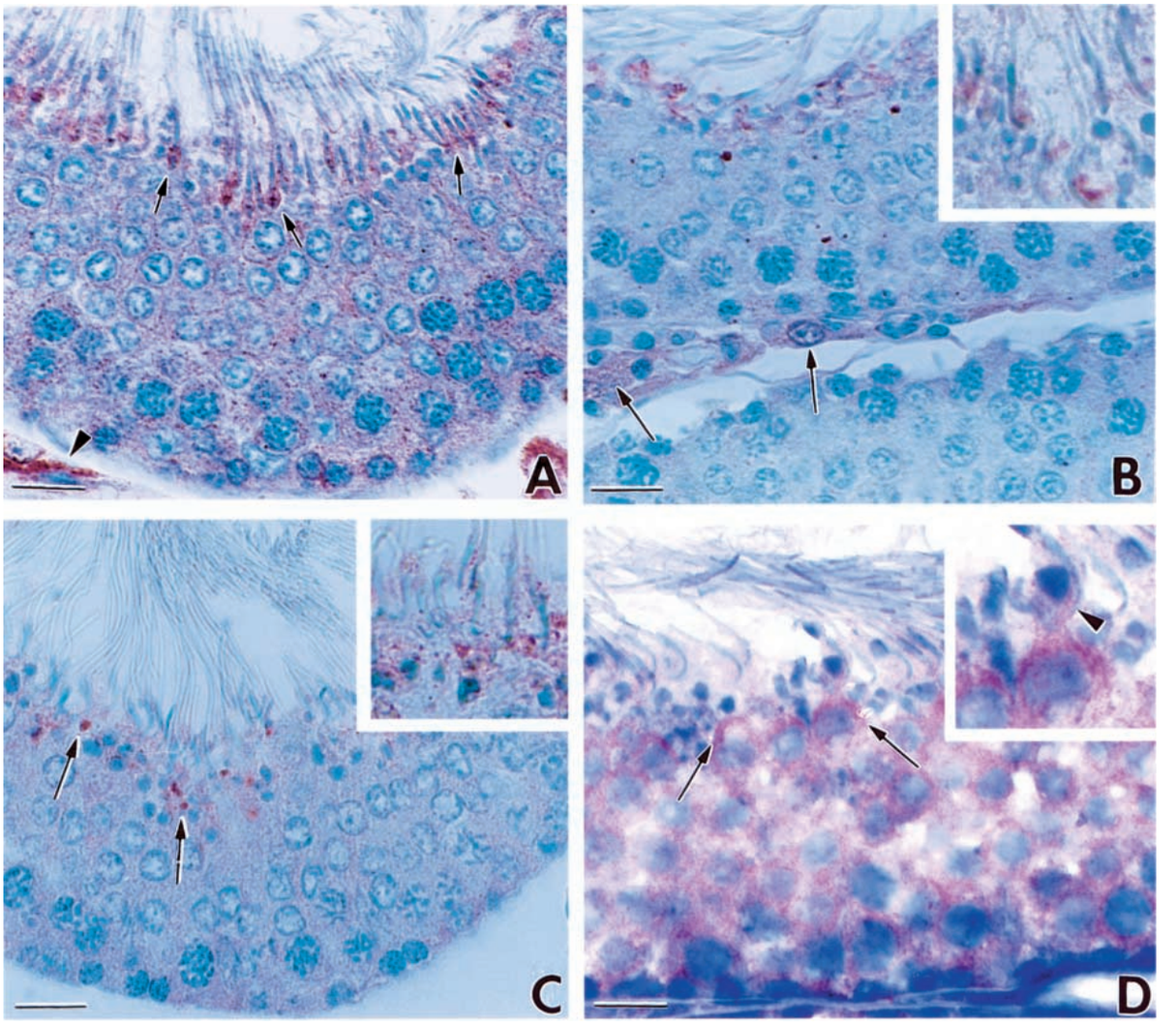

Figure 5. **(A)** CDC42 was not observed in peritubular cells, but appeared as diffuse granular staining in the cytoplasm of spermatocytes and spermatids. Staining was most intense around the heads of elongated spermatids (arrows) and in interstitial cells (arrowhead). Staining for serine phosphorylated proteins **(B)** stained cells in the interstitium (arrows) and cytoplasm around the heads of elongated spermatids (inset). Threonine-phosphorylated proteins also localized to the adluminal edge **(C)** as granular foci around residual bodies and mature spermatids (arrows). 14-3-3 Protein **(D)** appeared to be predominantly cytoplasmic, although some nuclear localization was observed at higher magnification. Staining intensity was greatest on the marginal edge of cells bordering the lumen (arrows), but rather faint in the cytoplasm surrounding mature spermatozoa. Chromogen granules can be seen in the residual cytoplasm being removed from mature spermatids prior to release from the epithelium (inset, arrowhead). Bar = 7.5 μm.

around and between the elongated spermatids and residual bodies (inset).

14-3-3 (FF)—The 14-3-3 family of proteins are found in signaling pathways in a broad range of organisms and tissues where they activate Raf family protein kinases (Berruti, 2000), regulate PKC (Jones et al, 1995), eventually leading to the activation of ERK1/2 downstream. In late stage VIII tubules (Figure 5D), antisera against 14-3-3 proteins stained as granulated foci in virtually all the cell types in the epithelium, with the exception of the peritubular cells. Prominent staining was noted in the cytoplasm of germ cells at the adluminal edge, as well as the cytoplasm of elongated spermatids (inset).

Coimmunoprecipitations

Each Western blot contained 4 lysates as positive controls: HeLa, human endothelial cell, rat brain, and whole rat testis. Two negative control reactions (omitting antiserum) using tubule lysates from before and after spermiation were also included in each experiment. Due to space considerations only one representative negative control lane is presented for each figure. Positive controls

have been omitted from the figures. Because often the same antigen was detected both before spermiation (BS) and after spermiation (AS), only one lane has been presented and labeled as BS/AS. Finally, prior to employing a primary antibody for use in a coimmunoprecipitation experiment, it was first tested for its ability to precipitate the antigen of interest. For example, we wondered whether antisera directed against *N*-cadherin would precipitate *N*-cadherin protein from precleared testis lysate. The results were verified by performing a Western blot for *N*-cadherin on the coimmunoprecipitation products from each *N*-cadherin antibody used. Data from these initial experiments have been omitted from the final results.

When examining the images, 4 points are important: 1) The heavy and light chains of the antibody often appear as bands in the figures, but always at a known molecular weight. 2) Because the luminescent images were collected digitally at a number of different magnifications, and each image presented here is a composite of numerous blots, occasionally the heavy and light chains of the antisera used in the coimmunoprecipitation reactions appear to be ''out of register'' (ie, at different molecular weights) across lanes. 3) In addition, to extend the amount of information that could be obtained from a single coimmunoprecipitation/Western blot experiment, primary antisera directed against more than one antigen were often combined in each Western blot, as long as the antigens were of sufficiently different molecular weights. 4) Each coimmunoprecipitation was performed at least 3 times, and only those coimmunoprecipitations that repeated clearly each time are presented. In each lane, the antigen of interest is circumscribed in white.

Western blots presented in Figure 6 show that antisera against *N*-cadherin precipitated β_1 integrin, α_4 integrin, cortactin, β-catenin, actin, Src, and pp120^{ctn}, both before and after spermiation. ILK was coprecipitated before spermiation only and β_1 integrin was the only protein identified as being coimmunoprecipitated with antisera to α_4 integrin.

Antisera against β-catenin coprecipitated *N*-cadherin and pp120^{ctn} both before and after spermiation. β_1 integrin and cortactin were coprecipitated before spermiation only, whereas ILK and actin were coprecipitated only after sperm release.

Antisera directed against vinculin coprecipitated β_1 integrin, pp120^{ctn}, and α_4 integrin both before and after spermiation whereas actin, ERK2, and a trace amount of ERK1 were detected after spermiation only.

Both before and after spermiation, antisera directed against paxillin coprecipitated β_1 integrin, α_6 integrin, cortactin, β-tubulin, actin, and pp120^{ctn}.

Proteins that coimmunoprecipitated with antiserum to cortactin were β_1 integrin, ILK, actin, paxillin, and ERK2, both before and after spermiation. No ERK1 was detected.

Antiserum to Src coprecipitated β-tubulin, cortactin, and ERK2, both before and after spermiation, yet actin was precipitated only after spermiation. Again, ERK1 was not precipitated with Src.

The immunohistochemical distribution of phosphorylated (active) ERK1/2 around the adluminal edge in stage VIII epithelia suggested the involvement of the MAP kinase pathway in the process of spermiation. This was further investigated by performing Western blots using anti-phosphoERK1/2 antiserum, and lysates prepared from tubules taken before, during, or after sperm release. For comparison, lysates were prepared from tubules treated with peroxovanadate, which is known to stimulate the MAP kinase pathway (Zhao et al, 1996), dosed at the same concentrations as described under the tubule culture methods above. Evident in Figure 7, phosphorylated ERK2 was detected at a uniform level in each of the tubule lysates. However, active ERK1 was detected only during spermiation, disappearing to trace amounts immediately after sperm release. In the peroxovanadate-treated samples, active ERK2 was detected in both control and low-dose-treated samples. Substantial activation of both ERK1 and ERK2 was observed in the peroxovanadate high dose lane.

Proteins Identified by Microsequencing

These methods were used to determine by sequencing which proteins coprecipitated with a known member of this putative multiprotein complex. Coimmunoprecipitations were performed using paxillin as the precipitating antisera followed by SAED cross-linking and mass spectrometry. Paxillin was chosen because it is believed to be responsible for the recruitment of structural and signaling molecules to focal adhesions (Turner, 1994; Brown et al, 1996), and was central in the model we proposed earlier (Wine and Chapin, 1999). A fluorescent band cut from gel at ≈118 kilodaltons (kd), was analyzed by MALDI. The resulting peptide mass data (not shown) was searched against the SwissProt database, which generated a list of matching proteins. The sample was further analyzed by Q-TOF, yielding a second set of peptide masses from which 4 strings of amino acid sequence were derived. Sequence search of SwissProt revealed that the unknown protein coprecipitated by paxillin was rat CD49f (α_6 integrin). Logistical considerations restricted the application to a single band. Western blots for threonine-phosphorylated proteins identified a band at ≈29 kd that showed a substantial increase in threonine phosphorylation during spermiation, which was not detected in the before or after spermiation (B/AS) lysates. A corresponding band cut from a Coomassie-stained gel, analyzed by MALDI/Q-

TOF yielded peptide fragments and sequence data that revealed the unknown protein to be rat 14-3-3 ζ.

Tubule Culture

All data given in the text are presented as the mean ± SD. Differences from the control (at $P < .05$) are indicated by *. After 16-20 hours in vitro, tubule sections had everted at both ends. Tails of adherent spermatids were visible under the dissecting microscope (Figure 8), whereas released sperm were visible in the medium. Microscopic evaluation of these sperm showed that they were without cytoplasm adherent to the head, although they did retain the cytoplasmic droplet along the tail. Release of sperm in untreated cultures appeared to depend on glutamine, as the percentage released under culture medium more than 6 weeks old decreased sharply, and was restored by adding fresh glutamine to the medium (data not shown). As more cultures were performed during the course of this work, the proportion of total sperm that were released rose erratically from the 30%–40% range to the 70%–80% range. In one experiment, we found that as segments for culture were taken further ''upstream'' from the point of spermiation (that is, earlier of stage VII and into stage VI), the percentage of sperm released into the medium sequentially declined: 47% ± 5.6% close to spermiation, 29.1% ± 10.7%, 24.4% ± 8.6%, and 13.9% ± 4.0% back into presumptive early VII or stage VI. When tubules were incubated with sodium azide (0.35 mg/2 mL), there was much less tubular eversion. Sperm release was reduced as well, from a control value of 33.7% ± 8.3% to *20.4% ± 10.0%. Azide-treated tubules had significant death of germ cells (clearly detectable histologically), although only ≈50% of the cells appeared affected. Sodium cyanide (1.7 mM) was less effective, but still reduced release by ≈30% (data not shown).

Three peroxovanadate experiments are summed and presented in Figure 9A. It shows a biphasic response: the lowest concentration of peroxovanadate reduces sperm release, whereas sequentially greater concentrations successively increase release.

Okadaic acid also shows an interesting, biphasic effect on sperm release (Figure 9B).

The effect of these 2 phosphatase inhibitors and the presence of an intense adluminal immunohistochemical signal for Src (Wine and Chapin, 1999), along with several related proteins, stimulated an evaluation of the possible involvement of tyrosine kinase activity in spermiation. Geldanamycin, which inhibits Src activity (Schnur et al, 1995) was used at 0.1, 0.3, 1.0, and 3.0 μM. Averaged over 4 geldanamycin experiments, the sperm release values (expressed as percent of control values for each experiment, and listed from lowest to highest concentrations [0.1–3.0 μM]) were 109% ± 16%, 81% ± 36%, 79% ± 5%, and 79% ± 7% of control. Other tyrosine kinase inhibitors were evaluated in limited experiments (1–3 dose levels, 3–4 wells per treatment, a single replicate). The data here are presented as the percentage of control release, with the low dose first: herbimycin A (0.01–0.1 μM) caused a 25% and 11% inhibition of release; H7 (1–100 μM) inhibited sperm release by 25%, 4%, and 17%. H8 (0.1–100 μM) inhibited sperm release by ≈21%, 20%, 26%, and 18%, whereas Lavendustin C (0.5, 5.0 μM) caused a 43% and 17% increase in sperm release. None of these changes significantly differ from control values; none of these tyrosine kinase inhibitors appeared to produce a profound inhibition of sperm release. Staurosporine, a broad-spectrum serine-threonine kinase inhibitor, was evaluated from 0.1–100 nM in log steps. Averaged data from 2 experiments are shown in Figure 9C. The same high-dose effect was seen consistently in several other experiments. The progressive dose-related decline in sperm release appears to provide compelling evidence for the involvement of Ser-Thr kinases in the process of spermiation. Because PKC is a serine/threonine kinase and Sertoli cells have PKC activity (Nikula et al, 1987), which are believed to be important in Sertoli cell–germ cell interaction (Ireland and Welsh, 1985), we evaluated the potential involvement of PKC in spermiation by evaluating 3 inhibitors of PKC. The average percent of control release values from 3 experiments each are as follows: bisindolylmaleimide 1 at 30 and 300 nM released 88.0% and 88.1% of the control value; the myristoylated PKC inhibitor 19–27 at 10 and 100 nM gave 91.2% and 94% of control release; RO-32-0432 at 60 and 600 nM gave 88.3% and 72.8% of control release. None of these significantly differ from control values, and we conclude that these data do not provide compelling evidence of PKC involvement in this process. When tubules were cultured in the EGF receptor blocker PD168393 at concentrations of 1, 10, 30, and 100 nM (2 experiments), the mean percentage of control release values were

→

Figure 6. Composite Western blots demonstrating the presence of various proteins in coimmunoprecipitates from seminiferous tubules before and after sperm release. An antibody to the protein under each composite was used as the precipitating antibody; those proteins that were coprecipitated with that antibody are listed across the top of each composite. Western blots were performed as described in ''Materials and Methods.'' In most experiments, more than one primary antibody was used, giving more than a single band in a lane. Multiple positive controls run in conjunction with the samples ensured the fidelity of the antibodies used. Due to space considerations and the large number of antisera used, the positive controls were not included in this figure. The protein of interest in each lane is encircled in white. The Table lists the source and molecular weight of the target antigen for each of the antisera used in this study. BS/AS indicates before spermiation/after spermiation.

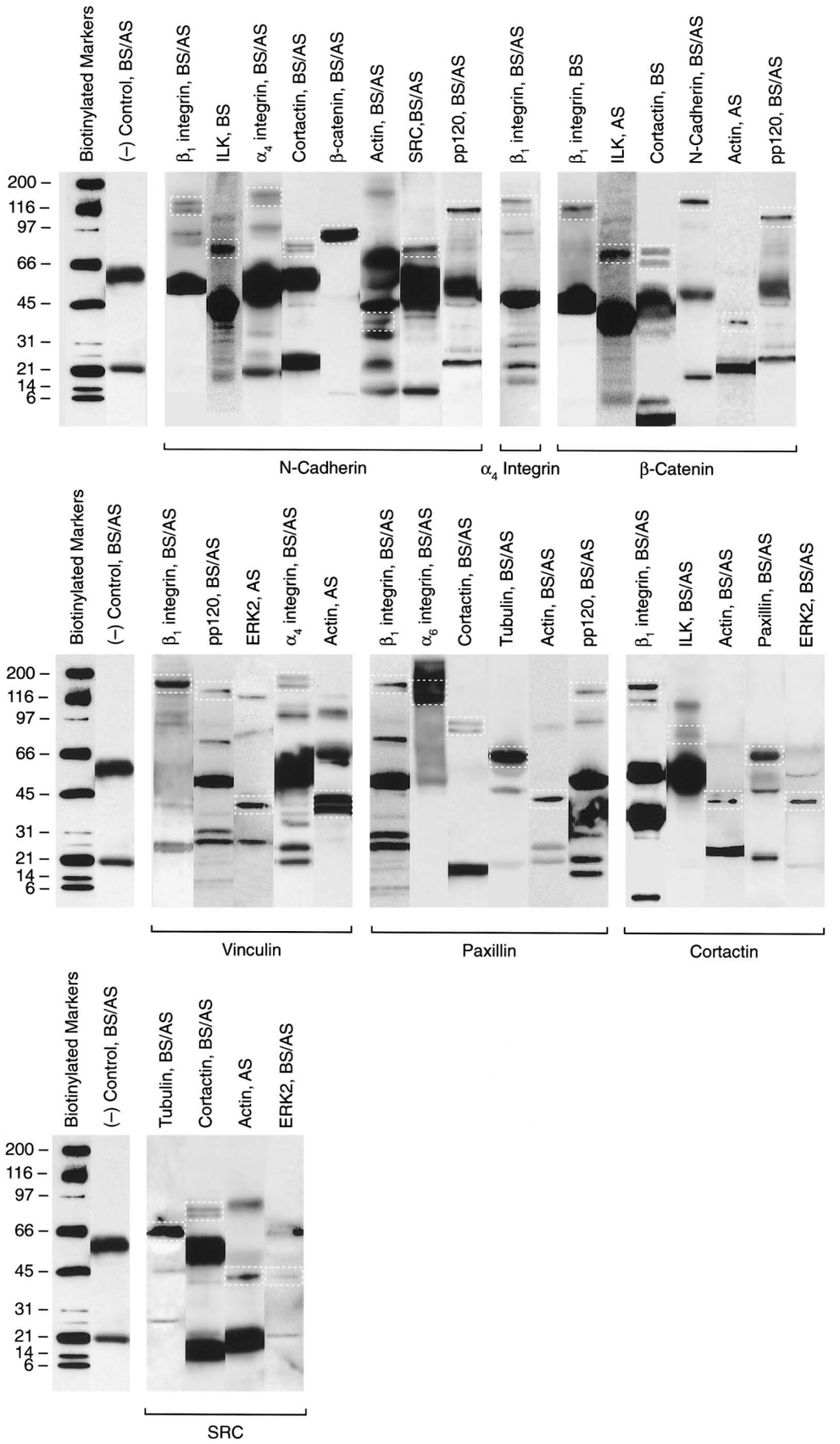
Biotinylated Markers
(–) Control, BS/AS
β1 integrin, BS/AS
ILK, BS
α4 integrin, BS/AS
Cortactin, BS/AS
β-catenin, BS/AS
Actin, BS/AS
SRC,BS/AS
pp120, BS/AS
β1 integrin, BS/AS
β1 integrin, BS
ILK, AS
Cortactin, BS
N-Cadherin, BS/AS
Actin, AS
pp120, BS/AS
200 –
116 –
97 –
66 –
45 –
31 –
21 –
14 –
6 –
N-Cadherin
α4 Integrin
β-Catenin
Biotinylated Markers
(–) Control, BS/AS
β1 integrin, BS/AS
pp120, BS/AS
ERK2, AS
α4 integrin, BS/AS
Actin, AS
β1 integrin, BS/AS
α6 integrin, BS/AS
Cortactin, BS/AS
Tubulin, BS/AS
Actin, BS/AS
pp120, BS/AS
β1 integrin, BS/AS
ILK, BS/AS
Actin, BS/AS
Paxillin, BS/AS
ERK2, BS/AS
Vinculin
Paxillin
Cortactin
Biotinylated Markers
(–) Control, BS/AS
Tubulin, BS/AS
Cortactin, BS/AS
Actin, AS
ERK2, BS/AS
SRC

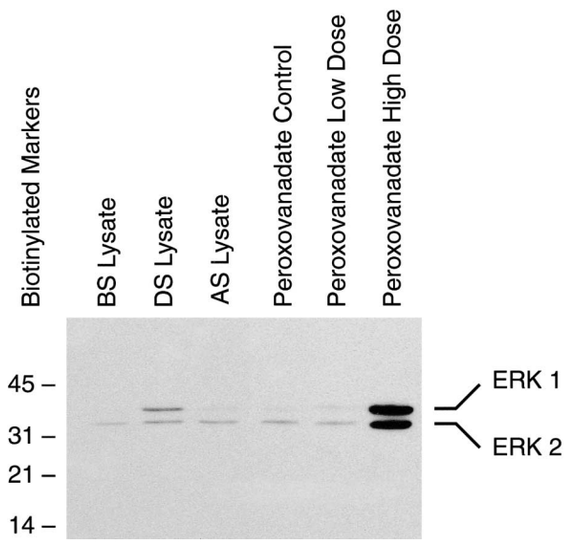

Figure 7. Western blot for phosphorylated ERK1/2 in seminiferous tubule lysates from before (BS), during (DS), and after (AS) spermiation, as well as following treatment with peroxovanadate. Equal amounts of protein were loaded into each lane. Active ERK1 was observed only during spermiation.

85.9%, 57.5%, 60%, and 89.5%, respectively. In addition, omitting EGF from the medium, or adding it at 10-fold the normal (3 ng/mL) level, had no effect on sperm release (not shown). It is interesting that varying FSH in the culture from none to a normal serum level (10 ng/mL) to 10-fold normal adult levels had no detectable effect in 2 separate experiments. This was done in conjunction with the EGF experiment above; there was no effect of varying EGF or FSH, and there was no interaction between the two hormones.

Finally, $\alpha_6\beta_1$ integrins have been localized to defined junctional structures that are believed to mediate spermatid-Sertoli adhesions (Salanova et al, 1995, 1998; Giebel et al, 1997). Bacitracin, an inhibitor of protein disulfide isomerase, has been shown to selectively inhibit β_1 and β_7 integrin mediated cell-cell adhesions in lymphocytes (Mou et al, 1998). Bacitracin (Figure 10) added to cultured seminiferous tubules at concentrations of 0.01 to 3.0 mM generated an increase in sperm release approximately 40%–60% over control values.

In summary, sperm release was significantly increased by bacitracin and relatively high concentrations of peroxovanadate and okadaic acid; sperm release was inhibited by staurosporine and relatively low concentrations of okadaic acid and peroxovanadate.

Discussion

These studies sought to further address the anatomy of a hypothetical multiprotein adhesion complex that was proposed earlier (Wine and Chapin, 1999). The proposed model was based on extensive immunohistochemical

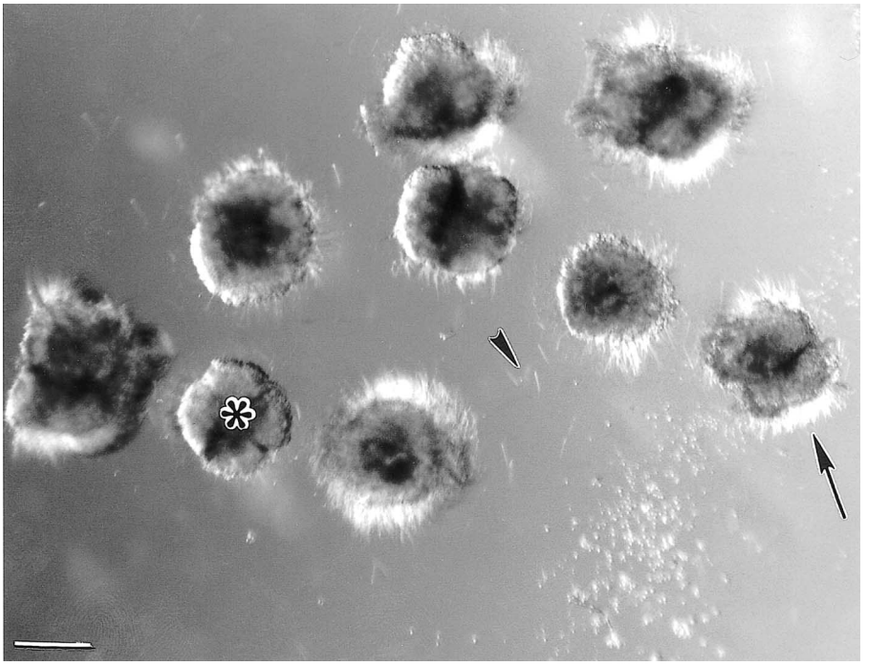

Figure 8. Transillumination photomicrograph of control tubules cultured for ≈16 hours. Note the apparent eversion, with tails of adherent sperm clearly visible (arrow). Individual sperm are also faintly visible at this power (arrowhead), although many more are visible throughout the well. Some tubules have released nearly all their sperm (asterisk). Bar = 100 μm.

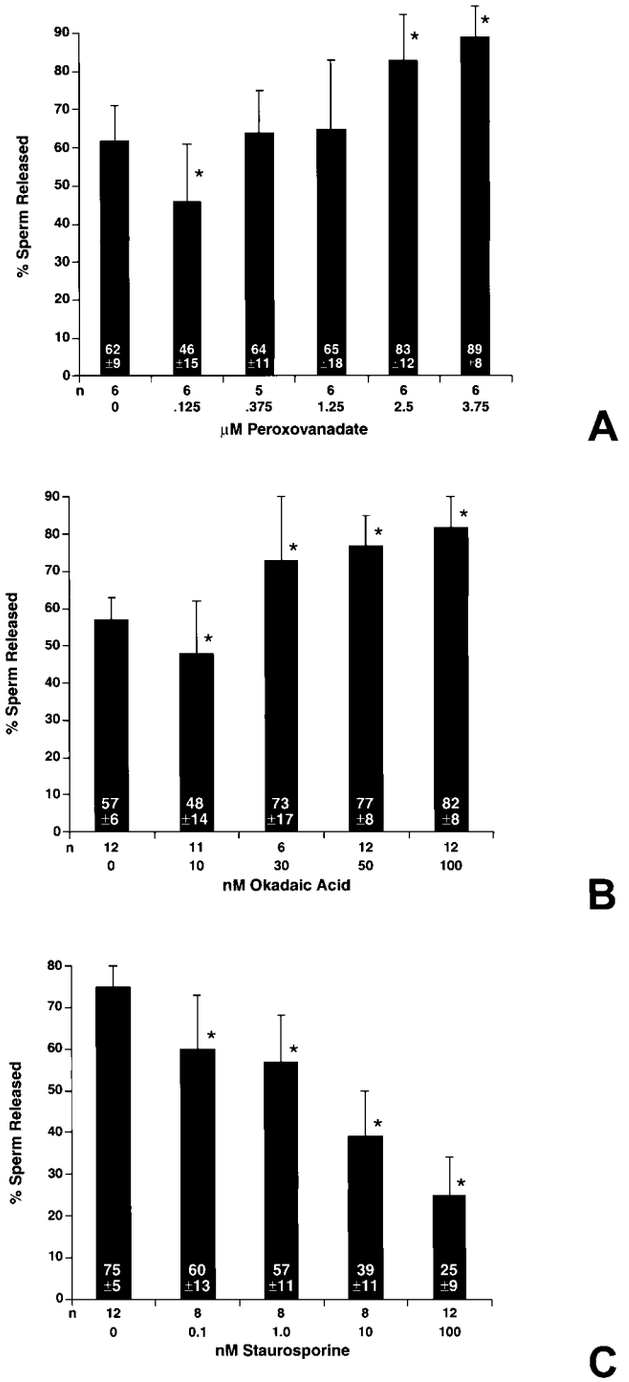

Figure 9. Summary graphs of the percentage of sperm release from tubule segments cultured for 16–20 hours in the presence of peroxovanadate **(A)**, okadaic acid **(B)**, or staurosporine **(C)**. Data are presented as mean ± SD. *Different from concurrent controls, $P < .05$.

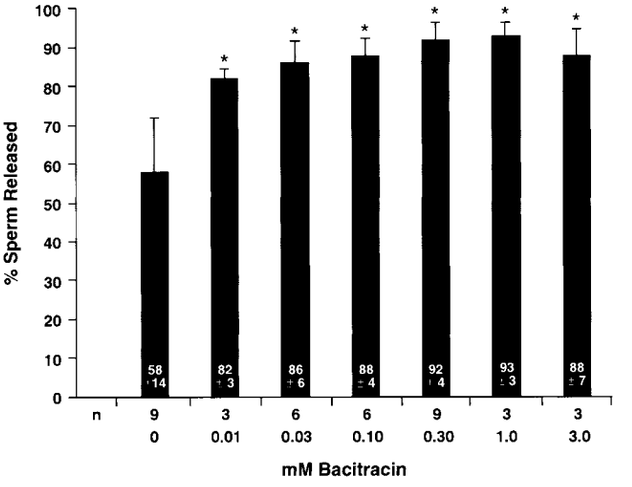

Figure 10. Summary graph of the percentage of sperm release from tubule segments cultured for 16–20 hours in the presence of bacitracin. Data are presented as mean ± SD. *Different from concurrent controls, $P < .05$.

evaluation performed in our laboratory and protein-protein interaction data published by other investigators, derived largely from cell culture models. In the current report, we have attempted to refine the previous model by determining which proteins are physically linked to one another in the seminiferous epithelium, and by identifying a few unknown proteins involved in the complex. Control of this model was tested by attempting to experimentally perturb the spermiation process in vitro, in a manner that would provide some insight into the mechanism or mechanisms of spermiation.

Based on extensive coimmunoprecipitation experiments and immunohistochemical data presented here and previously, a revised model of a multiprotein complex likely to be involved in the spermiation process is presented in Figure 11. Key features of this model are as follows: 1) *N*-cadherin is shown to be associated with at least 2 integrins, 2) several kinases are shown to be associated with other proteins in this complex, and 3) several proteins are known to regulate cytoskeletal function. This model sums data from 3 different methods: immunohistochemistry, showing that a protein is present adluminally at the time of spermiation; coimmunoprecipitation, showing that these proteins are linked; and in vitro tubule culture, which shows that ser-thr kinase inhibitors alter spermatid release, and a blocker of β_1 integrin function stimulates release.

Although all proteins in this report have immunohistochemistry and coimmunoprecipitation data to support their involvement in this process, the proteins with the greatest degree of data support appear to be β_1-integrin and the ser-thr kinases, because the tubule culture data show that inhibiting β_1 integrin function, or Ser-Thr kinase function, alter spermatid release.

Important procedural constraints limit the interpretation of these results:

1. It is clear that the level of resolution presented here

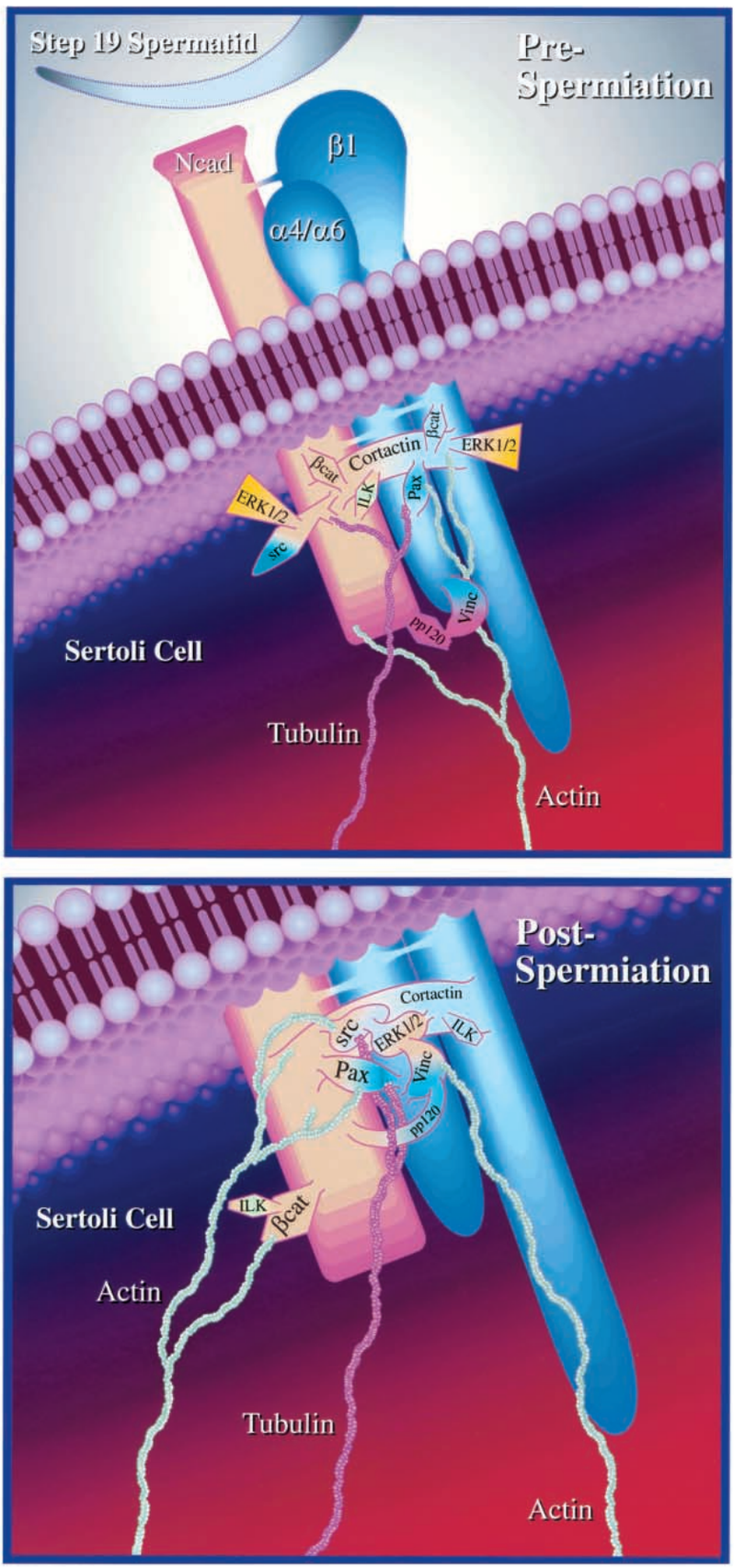
Step 19 Spermatid
Pre-
Spermiation
Ncad
β1
α4/α6
βcat
Cortactin
βcat
ERK1/2
ERK1/2
ILK
Pax
src
Vinc
pp120
Sertoli Cell
Tubulin
Actin
Post-
Spermiation
Cortactin
src
ERK1/2
ILK
Pax
Vinc
pp120
ILK
βcat
Sertoli Cell
Actin
Tubulin
Actin

does not allow for definitive assignment of many of these proteins to one cell type or another. However, several of these proteins (cortactin, Ras, RalA, and ERK1/2) clearly were around and not in residual bodies, consistent with Sertoli cell localization. Ultrastructural studies are needed to precisely confirm the cellular location of many of these proteins.

2. Many of these proteins were present at multiple places in the epithelium, and many junctions are being reformed at this time (ie, the basolateral Sertoli-Sertoli tight junctions, and the Sertoli–step 9 spermatid junctions). While the combined used of immunohistochemistry and coimmunoprecipitation and the evaluation of complexes before versus after spermiation were all used in an attempt to exclude these other junctions from this investigation, no method short of laser capture microdissection would truly remove all possible ''contamination'' by these other junctions. Thus, changes in these other junctions may be contributing to the data we report here.
3. The coimmunoprecipitation methods used here allow for the possibility that protein B, for example, may bridge between proteins A and C, and when precipitating with an antibody to protein A and probing only for protein C, we would miss the connecting protein B, and would erroneously conclude that proteins A and C were physically connected. So, we could be missing proteins that are present and serving an important role.
4. In addition, it is not completely impossible that proteins may coprecipitate even though they are not joined. However, we observed numerous other proteins at the luminal edge that were *not* coprecipitated in our experiments (eg, PKCμ, Csk, p38 MAP kinase), which strongly suggests that the likelihood of random false positives is quite small.
5. The heavy and light chains of the antisera used to precipitate protein complexes are routinely present in Western blots at 50 and 25 kd. Because Western blots were usually performed using a horseradish peroxidase-linked anti-mouse secondary antibody, these bands were normally and consistently detected in our blots. These bands may prevent the immunoprobing of blots for certain proteins; for example, the GTPase proteins (Rac1, RalA, etc.) are ≈21–25 kd, and are obscured by the antibody bands. As a result, these proteins may be present, but could not be evaluated, and therefore are not included in the proposed model.
6. Antibodies bind to certain surface motifs on a protein. If this same motif is the binding site for another cellular protein, and the antibody displaces that protein, the displaced protein will not be found in the precipitated complex.
7. Although the tubule culture provides an in vitro model that can be used to explore the events controlling spermiation, it comes with the limitations of all culture systems. For example, our data indicating that FSH in vitro was ineffective in modulating sperm release are inconsistent with the in vivo data of Saito et al (2000). They report that withdrawal of FSH and testosterone in vivo, over the course of 1 week, results in a ≈50% reduction in sperm release. Because the acute time frame of these cultures and the relatively long duration of hormone action, comparable hormone studies using tubule segments in vitro are unlikely without pretreatment of the animals.

A new hypothetical model for junctional adhesion and control molecules was recently proposed by Mulholland et al (2001), which includes $\alpha_6\beta_1$ integrin, ILK, actin, vinculin, paxillin, and suggests the involvement of small GTPases such as Rho. We have also found these same proteins in our protein complex, confirming at least this part of the molecular anatomy. In addition, their findings are extended by the demonstration of several additional proteins. Our data are also consistent with those of O'Donnell et al (2000), who showed vinculin, actin, and espin in or around the tubulobulbar complexes at spermiation. Their data suggest that espin could play a role in the model presented here.

Cortactin is an actin bundling protein that localizes to the cortical cytoskeleton, and has been shown to cross-link F-actin in vitro (Huang et al, 1997), a capability that was dramatically reduced by tyrosine phosphorylation. Actin is abundant at the adluminal edge, redistributing after sperm release (Vogl et al, 1985; Wine and Chapin, 1999); therefore, it makes sense that cortactin would be present here. Cortactin has been suspected of being involved in the transmission of signals from the membrane to the actin cytoskeleton, and several kinases are known to regulate cortactin activity, including Src, FYN, and FER (Kim and Wong, 1998).

The results of coimmunoprecipitation experiments presented here indicate that not only did cortactin coimmunoprecipitate Src both before and after spermiation, it also precipitated the MAP kinase ERK2, as well as ILK. The MAP kinases are a family of serine/threonine kinases that

←

Figure 11. Proposed model of protein complexes formed before (upper figure) and after spermiation. The model is based on immunohistochemical data presented in this manuscript and in published work from this laboratory (Wine and Chapin, 1999), in addition to extensive coimmunoprecipitation studies. Points of contact between the different proteins indicate that these proteins coimmunoprecipitated with one another in vitro. Examination of the model reflects the substantial rearrangement of proteins that occurs after sperm release.

regulate a broad range of cellular activities. One class of the MAP kinases is the ERKs, of which there are 2 major isoforms, p44 (ERK1) and p42 (ERK2). ERK1/2 and its kinase (MEK) operate downstream of Ras proteins to affect transcription (see Seger and Krebs, 1995; Yamamoto et al, 1999). ILK has been suggested as one of the major kinases responsible for serine and threonine phosphorylation in focal adhesions (Li et al, 1999). The model we propose here includes both adhesion molecules and intracellular kinase regulators of adhesion and cytoskeletal architecture, consistent with events known to occur at the luminal edge of the seminiferous epithelium.

One of the more intriguing findings of these studies has been the repeated coimmunoprecipitation of *N*-cadherin and integrin $\alpha_4\beta_1$. Whereas to our knowledge this previously has not been documented in the testis, the interaction and regulation of cadherins by integrins has been demonstrated in other cell types (Higgins et al, 1998; Gimond et al, 1999; Celetti et al, 2000; Kawano et al, 2001). In neural crest cells, Monier-Gavelle, et al (1997) reported evidence of the control of *N*-cadherin by the activity of β_1 and β_3 integrin, providing another example of cross-talk between these adhesion molecules. The interaction between cadherins and integrins suggests multiple pathways of control of these junctions, and also leads to the following hypothesis: By mixing different types of adhesion molecules, different generations of germ cells may signal their presence to Sertoli cells, possibly triggering any specialized support or secretory functions of the Sertoli cell.

Multiple methods of control suggest many possible targets for toxicant action, which is consistent with the experience that disrupted spermiation is observed following a wide variety of toxicant exposures. The logical next step in this exploration would be to determine which proteins are phosphorylated during spermatid release, and then treating animals with release-disrupting toxicants, and determining alterations in that pattern of phosphorylation. Our prediction is that different toxicants will alter the phosphorylation of different combinations of these proteins.

The distribution of β_1 integrin has been previously documented in rat seminiferous epithelium (Palombi et al, 1992; Salanova et al, 1995). Previous attempts to replicate the reported β_1 integrin distribution in our laboratory failed (Wine and Chapin, 1999). In this current work, using anti-β_1 integrin antisera from a particular manufacturer (Chemicon, Inc, Temecula, Calif) and paraformaldehyde-fixed/antigen retrieved tissue, we were able to reproduce the protein distribution previously documented by others. Although we were able to detect β_1 integrin by Western blotting in coimmunoprecipitation lysates using antibodies directed against other proteins, and were able to precipitate β_1 integrin itself, numerous attempts to effect a coimmunoprecipitation with this antibody were unsuccessful. This is neither surprising nor troubling because not all antibodies are capable of immunoprecipitating their antigen proteins.

In our hands, bacitracin, even at its lowest dose (0.01 nM), significantly increased the percentage of sperm release in vitro. Demonstrated to interfere with both β_1 and $\alpha_4\beta_7$ integrin-mediated adherence in lymphoid cells (Mou et al, 1998), the precise mechanism by which bacitracin disrupts integrin-dependent cell adhesion is not known. If bacitracin's effect on β_1 integrin functionality is believed to be the mechanism for induced release, these data demonstrate a role for β_1 integrin in adhesion, and validate the utility of an in vitro tubule culture model.

Although low doses of okadaic acid (30–100 nM) initially inhibited sperm release, incubation of tubules with the phosphatase inhibitor resulted in a significant increase in the release of sperm into the surrounding medium. This increase in release may also be occurring via β_1 integrin. Recent work by Mulrooney et al (2000) reports that parietal endoderm treated with okadaic acid induced an increase in β_1 integrin phosphorylation, resulting in a selective loss of β_1 integrin from focal adhesion sites. Furthermore, ILK was shown to coimmunoprecipitate with β_1 integrin, localize to focal adhesions, and okadaic acid treatment significantly decreased the level of ILK associated with β_1 integrin.

α integrin cytoplasmic domains are important for regulation of integrin function, and different α subunits differentially regulate integrin-mediated responses (Sastry and Horwitz, 1993). In our hands, α_4 integrin was precipitated with both *N*-cadherin and vinculin. However, of the different proteins examined, only β_1 integrin was precipitated by α_4 integrin antisera. Although α_4 and α_6 integrin shared similarities in immunohistochemical distribution, differences in molecular weight detected by Western blotting (150/80 kd and 118 kd, respectively), and sequence alignment showing only 38% similarity between the two proteins, suggest a lack of antisera cross-reactivity.

Despite our findings for α_4 integrin, $\alpha_6\beta_1$ seems the most likely integrin heterodimer involved in the spermiation process. We initially found that integrin α_6 coimmunoprecipitated with paxillin by MALDI/Q-TOF, a finding subsequently verified by Western blotting. Evidence of an interaction between the intracellular region of the integrin β_1 subunit and paxillin in vitro has been previously reported (Tanaka et al, 1996). In addition, Shaw et al (1995) reported α_6 tail-induced integrin-dependent paxillin phosphorylation. Despite numerous attempts, we were unable to detect α_6 integrin in coimmunoprecipitations using antisera to other proteins.

In our hands, ILK coimmunoprecipitated with cortactin both before and after sperm release, suggesting a stable association between the two proteins (Figure 6). Others

have reported that overexpression of constitutively active ILK results in a loss of cell-cell adhesion (Novak et al, 1998). The finding of a close association between cortactin and ILK, and the interaction of ILK with β_1 integrin, provides both a mechanical linkage of the integrin β chain to the cytoskeleton, and to a signal transduction mechanism, perhaps through β-catenin. This is consistent with other recent advances made in the attempt to elucidate the molecular mechanisms of integrin-mediated bidirectional signal transduction (for a review, see Liu et al, 2000).

The distribution of ERK1/2 in the testis and the activation of both ERK isoforms during the time of sperm release (Figure 7) intrigued us. Activation of the MAP kinase pathway by Ras has been shown by others to be required for junctional disassembly (Potempa and Ridley, 1998), and numerous observations have demonstrated that integrin-mediated cell anchorage can regulate the efficiency of signaling from receptor tyrosine kinase to MAP kinase (Short et al, 2000). ERK2 was the predominant isoform coimmunoprecipitated with cortactin both before and after sperm release. However, ERK2 (and trace amounts of ERK1) were detected in vinculin coimmunoprecipitations only after spermiation. In addition to the ERKs, we noted that actin also coimmunoprecipitated with vinculin only after spermiation, showing a rearrangement of proteins, perhaps the result of MAP kinase activation.

Further involvement of the ERK/MAP kinase pathway is supported by Western blots using anti-phospho-threonine antisera and MALDI/Q-TOF. 14-3-3 ζ was identified by mass spectrometry/mass spectrometry (MS/MS) as the threonine-phosphorylated band that appeared only in lysates of tubule segments during sperm release. Identified in the testis by others (Perego and Berruti, 1997), the highly conserved 14-3-3 family of proteins are believed to function as regulators of diverse signaling pathways. One isoform identified in the testis, 14-3-3 θ, has been suggested to influence Sertoli cell function (Chaudhary and Skinner, 2000), and has been found as a complex with Rap1 and B-Raf, which function upstream of the ERK/MAP kinase pathway (Berruti, 2000). Because 14-3-3 ζ was not further examined by coimmunoprecipitation, its relationship with other proteins in our model could not be determined. For this reason it was not included in the final model.

The tubule culture model used in this study proved to be a valuable tool for testing a number of pharmacological agents, and whose absence has been recognized as a shortcoming in testing proposed models. Collectively, the data did not strongly support the involvement of tyrosine kinases, but did suggest the involvement of serine/threonine kinase activity. Treatment of tubule segments with the serine/threonine kinase inhibitor staurosporine resulted in a significant decrease in sperm release in a dose-dependent fashion. Conversely, treatment with peroxovanadate, a phosphatase inhibitor that also activates ERK1/2 (Zhao et al, 1996), increased sperm release in vitro. Activation of ERK1/2 by peroxovanadate was confirmed by Western blotting (Figure 7), which also revealed ERK1 activation at the time of sperm release in untreated control tubules.

Those results from the tubule culture model prompted us to localize serine/threonine phosphoproteins using immunohistochemistry. The presence of Ser-Thr phosphoprotein immunostaining at the adluminal edge, together with the in vitro data and the identification of 14-3-3 ζ by MS/MS, collectively provide strong evidence for serine-threonine phosphorylation as a key event in spermiation, and in particular the ERK/MAP kinase pathway.

A number of questions remain unanswered and beg further investigation:

1. What is the precise role of 14-3-3 ζ in the spermiation process and how does it interact with or influence other signal transduction pathways in the testis?
2. Are the small GTPases present and involved?
3. Given the compelling evidence for the involvement of the ERK/MAP kinase pathway provided here, but the fact that the regulation of this pathway appears different from that in other cells, an in-depth study of the function and regulation of this signaling pathway in the spermiation process is needed.
4. While stage-specific tubule dissection has helped to focus coimmunoprecipitations to before, during, or after sperm release, we have relied on immunohistochemistry to infer where in the Sertoli cell the specific proteins are interacting. More precise methods of tissue isolation, such a laser assisted microdissection, in conjunction with protein cross-linking and coimmunoprecipitation, could be used to more directly examine protein-protein interaction at the adluminal edge.

Despite the interpretational limitations, the caveats, and the unanswered questions, these data provide new insight and hypotheses into the molecular structures and mechanisms underlying spermiation and provide fertile ground for many future investigations. The complexity of the multiprotein structure is not surprising, given the multifactorial nature of its job. That complexity also provides many targets for toxicants and thus helps explain why this process is a common target for numerous structurally diverse toxicants.

In summary, the results of the coimmunoprecipitation/Western blot data and immunohistochemistry have been combined to generate a revised model of a junctional protein complex. This model refines and extends models proposed earlier (Wine and Chapin, 1999; Mulholland et al, 2001), and together with the tubule culture data, supports

the involvement of serine/threonine kinases and β_1 integrin in the release process. Future work in this area will continue to refine and improve this model and yield more exciting insights into the control of this critical process.

Acknowledgments

The authors are grateful to Drs Kamin Johnson, Liza O'Donnell, and Wayne Vogl for their helpful comments and review of this manuscript. We are also grateful to Steve Edgerton of Image Associates for his unsurpassed skill in creating the figure of the protein model. Finally, we are forever indebted to the animals whose sacrifice made this work possible.

References

Berruti G. A novel Rap1/B-Raf/14-3-3 θ protein complex is formed in vivo during the morphogenetic determination of postmeiotic male germ cells. *Exp Cell Res.* 2000;257:172–179.

Borchers C, Peter JF, Hall MC, Kunkel TA, Tomer KB. Identification of in-gel digested proteins by complementary peptide mass fingerprinting and tandem mass spectrometry data obtained on an electrospray ionization quadrupole time-of-flight mass spectrometer. *Anal Chem.* 2000;76:1163–1168.

Borchers C, Tomer KB. Characterization of the noncovalent complex of human immunodeficiency virus glycoprotein 120 with its cellular receptor cd4 by matrix-assisted laser desorption/ionization mass spectrometry. *Biochemistry.* 1999;38:11734–11740.

Bowden ET, Barth M, Thomas D, Glazer RI, Mueller SC. An invasion-related complex of cortactin, paxillin and PKCμ associates with invadopodia at sites of extracellular matrix degradation. *Oncogene.* 1999;18:4440–4449.

Braga V. Epithelial cell shape: cadherins and small GTPases. *Exp Cell Res.* 2000;261:83–90.

Braga VM. Small GTPases and regulation of cadherin dependent cell-cell adhesion. *Mol Pathol.* 1999;52:197–202.

Braga VMM, Machesky LM, Hall A, Hotchin NA. The small GTPases Rho and Rac are required for the establishment of cadherin-dependent cell-cell contacts. *J Cell Biol.* 1997;137:1412–1431.

Brown MC, Perrotta JA, Turner CE. Identification of LIM3 as the principal determinant of paxillin focal adhesion localization and characterization of a novel motif on paxillin directing vinculin and focal adhesion kinase binding. *J Cell Biol.* 1996;135:1109–1132.

Burridge K. Crosstalk between Rac and Rho. *Science.* 1999;283:2028–2029.

Byers SW, Jégou B, MacCalman C, Blaschuk O. Sertoli cell adhesion molecules and the collective organization of the testis. In: Russell LD, Griswold MD, eds. *The Sertoli Cell.* Clearwater, Fla: Cache River Press; 1993:461–476.

Celetti A, Garbi C, Consales C, Cerrato A, Greco D, Mele E, Nitsch L, Grieco M. Analysis of cadherin/catenin complexes in transformed thyroid epithelial cells: modulation by beta 1 integrin subunit. *Eur J Cell Biol.* 2000;79:583–593.

Chaudhary J, Skinner MK. Characterization of a novel transcript of 14-3-3 theta in Sertoli cells. *J Androl.* 2000;21:730–738.

Chen HC, Appeddu PA, Parsons JT, Hildebrand JD, Schaller MD, Guan JL. Interaction of focal adhesion kinase with cytoskeletal protein talin. *J Biol Chem.* 1995;270:16995–16999.

Chen L-M, Bailey D, Fernandez-Valle C. Association of β_1 integrin with focal adhesion kinase and paxillin in differentiating Schwann cells. *J Neurosci.* 2000;20:3776–3784.

Collares-Buzato CB, Jepson MA, Simmons NL, Hirst BH. Increased tyrosine phosphorylation causes redistribution of adherens junction and tight junction proteins and perturbs paracellular barrier function in MDCK epithelia. *Eur J Cell Biol.* 1998;76:85–92.

Couldwell WT, Hinton DR, He S, Chen TC, Sebat I, Weiss MH, Law RE. Protein kinase C inhibitors induce apoptosis in human malignant glioma cell lines. *FEBS Lett.* 1994;345:43–46.

Delcommenne M, Tan C, Gray V, Rue L, Woodgett J, Dedhar S. Phosphoinositide-3-OH kinase-dependent regulation of glycogen synthase kinase 3 and protein kinase B/AKT by the integrin-linked kinase. *Proc Natl Acad Sci USA.* 1998;95:11211–11216.

Fröjdman K, Pelliniemi LJ. Differential distribution of the α_6 subunit of integrins in the development and sexual differentiation of the mouse testis. *Differentiation.* 1994;57:21–29.

Giebel J, Löster K, Rune GM. Localization of integrin β_1, α_1, α_5 and α_9 subunits in the rat testis. *Int J Androl.* 1997;20:3–9.

Gimond C, van der Flier A, van Delft S, Brakebusch C, Kuikman I, Collard JG, Fässler R, Sonnenberg A. Induction of cell scattering by expression of β_1 integrins in β_1 deficient epithelial cells requires activation of members of the Rho family of GTPases and downregulation of cadherin and catenin function. *J Cell Biol.* 1999;147:1325–1340.

Gjertsen BT, Cressey LI, Ruchaud S, Houge G, Lanotte M, Døskeland SO. Multiple apoptotic death types triggered through activation of separate pathways by cAMP and inhibitors of protein phosphatases in one (IPC leukemia) cell line. *J Cell Sci.* 1994;107:3363–3377.

Grove BD, Vogl AW. Sertoli cell ectoplasmic specializations: a type of actin-associated adhesion junction? *J Cell Sci.* 1989;93:309–323.

Gumbiner BM. Regulation of cadherin adhesive activity. *J Cell Biol.* 2000;148:399–403.

Hannigan GE, Leung-Hagesteijn C, Fitz-Gibbon L, Coppolino MG, Radeva G, Filmus J, Bell JC, Dedhar S. Regulation of cell adhesion and anchorage dependent growth by a new beta-1 integrin linked protein kinase. *Nature (Lond).* 1996;379:91–96.

Haystead TAJ, Sim ATR, Carling D, Honnor RC, Tsukitani Y, Cohen P, Hardie DG. Effects of the tumor promoter okadaic acid on intracellular protein phosphorylation and metabolism. *Nature.* 1989;337:78–81.

Higgins JMG, Mandlebrot DA, Shaw SK, et al. Direct and regulated interaction of integrin $\alpha_E\beta_7$ with E-cadherin. *J Cell Biol.* 1998;140:197–210.

Huang C, Ni Y, Wang T, Gao Y, Haudenschild CC, Zhan X. Down-regulation of the filamentous actin cross-linking activity of cortactin by Src-mediated tyrosine phosphorylation. *J Biol Chem.* 1997;272:13911–13915.

Inagaki K, Noguchi T, Matozaki T, Horikawa T, Fukunaga K, Tsuda M, Ichihashi M, Kasuga M. Roles for the protein tyrosine phosphatase SHP-2 in cytoskeletal organization, cell adhesion and cell migration revealed by overexpression of a dominant negative mutant. *Oncogene.* 2000;19:75–84.

Ireland ME, Welsh MJ. Germ cell stimulation of Sertoli cell protein. *Endocrinology.* 1985;120:1317–1325.

Jockusch BM, Bubeck P, Giehl K, et al. The molecular architecture of focal adhesions. *Ann Rev Cell Dev Biol.* 1995;11:379–416.

Johnson KJ, Hall ES, Boekelheide K. 2,5 Hexanedione exposure alters the rat Sertoli cell cytoskeleton. I. Microtubes and seminiferous tubule fluid secretion. *Toxicol Appl Pharmacol.* 1991;111:432–442.

Johnson KJ, Patel SR, Boekelheide K. Multiple cadherin superfamily members with unique expression profiles are produced in rat testis. *Endocrinology.* 1999;141:675–683.

Jones DHA, Martin H, Madrazo J, et al. Expression and structural analysis of 14-3-3 proteins. *J Mol Biol.* 1995;245:375–384.

Kamata T, Puzon W, Takada Y. Identification of putative ligand-binding sites of the integrin α_4/β_1 (VLA-4, CD49d/CD29). *Biochem J.* 1995;305:945–951.

Kawano K, Kantak SS, Murai M, Yao CC, Kramer RH. Integrin al-

pha3beta1 engagement disrupts intercellular adhesion. *Exp Cell Res.* 2001;262:180–196.

Kim L, Wong TW. Growth factor-dependent phosphorylation of the actin-binding protein cortactin is medicated by the cytoplasmic tyrosine kinase FER. *J Biol Chem.* 1998;273:23542–23548.

Kinghorn EM, Bate AS, Higgins SJ. Growth of rat seminal vesicle epithelial cells in culture: neurotransmitters are required for androgen-regulated synthesis of tissue-specific secretory proteins. *Endocrinology.* 1987;121:1678–1688.

Kjøller L, Hall A. Signaling to Rho GTPases. *Exp Cell Res.* 1999;253: 166–179.

Kuroda S, Fukata M, Nakagawa M, Kaibuchi K. Cdc42, Rac 1, and their effector IQGAP1 as molecular switches for cadherin-mediated cell-cell adhesion. *Biochem Biophys Res Com.* 1999;262:1–6.

Laemmli UK. Cleavage of structural proteins during the assembly of the head of bacteriophage T4. *Nature.* 1970;277:680–688.

Li F, Zhang Y, Wu C. Integrin-linked kinase is localized to cell-matrix focal adhesions but not cell-cell adhesion sites and the focal adhesion localization of integrin-linked kinase is regulated by the PINCH-binding ANK repeats. *J Cell Sci.* 1999;112:4589–4599.

Li L, Wine RN, Miller DS, Reece JM, Smith M, Chapin RE. Protection against methoxyacetic-acid-induced spermatocyte apoptosis with calcium channel blockers in cultured rat seminiferous tubules: possible mechanisms. *Toxicol Appl Pharmacol.* 1997;144:105–119.

Liu S, Calderwood DA, Ginsberg MH. Integrin cytoplasmic domain-binding proteins. *J Cell Sci.* 2000;113:3563–3571.

Mallea LE, Machado AJ, Navoroli F, Romments FFG. Epidermal growth factor stimulates lactate production and inhibits aromatization in cultured Sertoli cells from immature rats. *Int J Androl.* 1986;9:201–208.

Maruyama S, Kurosaki T, Sada K, Yamanashi Y, Yamamoto T, Yamamura H. Physical and functional association of cortactin with Syk in human leukemic cell line K562. *J Biol Chem.* 1996;271:6631–6635.

Means AR, Dedman JR, Fakunding JL, Tindall DJ. Mechanism of action of FSH in the male rat. In: Birnbaumer L, O'Malley BW, eds. *Receptors in Hormone Action.* Vol. 3. New York, NY: Academic Press; 1978:363–392.

Mimnaugh EG, Chavany C, Neckers L. Polyubiquitination and proteasomal degradation of the $p185^{c\text{-}erbB\text{-}2}$ receptor protein-tyrosine kinase induced by geldanamycin. *J Biol Chem.* 1996;271:22796–22801.

Monier-Gavelle F, Duband J-L. Cross talk between adhesion molecules: control of *N*-cadherin activity by intracellular signals elicited by β_1 and β_3 integrins in migrating neural crest cells. *J Cell Biol.* 1997;137: 1663–1681.

Mou Y, Ni H, Wilkins JA. The selective inhibition of β_1 and β_7 integrin-mediated lymphocyte adhesion by bacitracin. *J Immunol.* 1998;161: 6323–6329.

Mulholland DJ, Dedhar S, Vogl AW. Rat seminiferous epithelium contains a unique junctional (ectoplasmic specialization) with signaling properties both of cell/cell and cell/matrix junctions. *Biol Reprod.* 2001;64:396–407.

Mulrooney J, Foley K, Vineberg S, Barreuther M, Grabel L. Phosphorylation of the β_1 integrin cytoplasmic domain: toward an understanding of function and mechanism. *Exp Cell Res.* 2000;258:332–341.

Nikula H, Naor Z, Parvinen M, Huhtaniemi I. Distribution and activation of protein kinase C in the rat testis tissue. *Mol Cell Endocrinol.* 1987; 49:39–49.

Novak A, Hsu S, Leung-Hagesteijn C, et al. Cell adhesion and the integrin-linked kinase regulate the LEF-1 and β-catenin signaling pathways. *Proc Natl Acad Sci USA.* 1998;95:4374–4379.

O'Donnell L, Stanton PG, Bartles JR, Robertson DM. Sertoli cell ectoplasmic specializations in the seminiferous epithelium of the testosterone-suppressed adult rat. *Biol Reprod.* 2000;63:99–108.

Oka S, Kodama M, Takeda H, Tomizuka N, Suzuki H. Staurosporine, a potent platelet aggregation inhibitor from a *Streptomyces* species. *Agric Biol Chem.* 1986;50:2723–2727.

Oko R, Hermo L, Hecht NB. Distribution of actin isoforms within cells of the seminiferous epithelium of the rat testis: evidence for a muscle form of actin in spermatids. *Anat Rec.* 1991;231:63–81.

Palombi F, Salanova M, Tarone G, Farini D, Stefanini M. Distribution of β_1 integrin subunit in rat seminiferous epithelium. *Biol Reprod.* 1992; 47:1173–1182.

Parvinen M, Toppari J, Lahdetie J. Transillumination-phase-contrast microscopic techniques for evaluation of male germ cell toxicity and mutagenicity. *Methods Toxicol.* 1993;3A:142–165.

Perego L, Berruti G. Molecular cloning and tissue-specific expression of the mouse homologue of the rat brain 14-3-3 θ protein: characterization of its cellular and developmental pattern of expression in the male germ line. *Mol Reprod Dev.* 1997;47:370–379.

Potempa S, Ridley AJ. Activation of both MAP kinase and phosphatidylinositide 3-kinase by Ras is required for hepatocyte growth factor/scatter factor-induced adherens junction disassembly. *Mol Biol Cell.* 1998;9:2185–2200.

Ruff SJ, Chen K, Cohen S. Peroxovanadate induces tyrosine phosphorylation of multiple signaling proteins in mouse liver and kidney. *J Biol Chem.* 1997;272:1263–1267.

Saito K, O'Donnell L, McLachlan RI, Robertson DM. Spermiation failure is a major contributor to early spermatogenic suppression caused by hormone withdrawal in adult rats. *Endocrinology.* 2000;141:2779–2785.

Salanova M, Ricci G, Boitani C, Stefanini M, De Grossi S, Palombi F. Junctional contacts between Sertoli cells in normal and aspermatogenic rat seminiferous epithelium contain $\alpha_6\beta_1$ integrins, and their formation is controlled by follicle-stimulating hormone. *Biol Reprod.* 1998;58:371–378.

Salanova M, Stefanini M, de Curtis I, Palombi F. Integrin receptor $\alpha_6\beta_1$ is localized at specific sites of cell-to-cell contact in rat seminiferous epithelium. *Biol Reprod.* 1995;52:79–87.

Sastry SK, Horwitz AF. Integrin cytoplasmic domains: mediators of cytoskeletal linkages and extra- and intracellular initiated transmembrane signaling. *Curr Opin Cell Biol.* 1993;5:819–831.

Schaller J, Glander HJ, Dethloff J. Evidence of β_1 integrins and fibronectin on spermatogenic cells in human testis. *Hum Reprod.* 1993;8: 1873–1878.

Schnur RC, Corman ML, Gallaschun RJ, et al. Inhibition of the oncogene product p185erbB-2 in vitro and in vivo by geldanamycin and dihydrogeldanamycin derivatives. *J Med Chem.* 1995;38:3806–3812.

Seger R, Krebs EG. The MAPK signaling cascade. *FASEB J.* 1995;9: 726–735.

Shaw LM, Turner CE, Mercurio AM. The $\alpha_6A\beta_1$ and $\alpha_6B\beta_1$ integrin variants signal differences in the tyrosine phosphorylation of paxillin and other proteins. *J Biol Chem.* 1995;270:23648–23652.

Short SM, Boyer JL, Juliano RL. Integrins regulate the linkage between upstream and downstream events in G protein-coupled receptor signaling to mitogen-activated protein kinase. *J Biol Chem.* 2000;275: 12970–12977.

Tanaka T, Yamaguchi R, Sabe H, Sekiguchi K, Healy JM. Paxillin association in vitro with integrin cytoplasmic domain peptides. *FEBS Lett.* 1996;399:53–58.

Trübner M, Glander H-J, Schaller J. Localization of adhesion molecules on human spermatozoa by fluorescence microscopy. *Andrologia.* 1997;29:253–260.

Turner CE. Paxillin: a cytoskeletal target for tyrosine kinases. *Bioessays.* 1994;16:47–52.

Vogl AW, Pfeiffer DC, Mulholland D, Kimel G, Guttman J. Unique and multifunctional adhesion junctions in testis: ectoplasmic specializations. *Arch Histol Cytol.* 2000;63:1–15.

Vogl AW, Soucy LJ. Arrangement and possible function of actin filament

bundles in ectoplasmic specializations of ground squirrel Sertoli cells. *J Cell Biol.* 1985;100:814–825.

Vogl AW, Soucy LJ, Lew GJ. Distribution of actin in isolated seminiferous epithelia and denuded tubule walls of the rat. *Anat Rec.* 1985; 213:63–71.

Vojtek AB, Cooper JA. Rho family members: activators of MAP kinase cascades. *Cell.* 1995;82:527–529.

Wine RN, Chapin RE. Adhesion and signaling proteins spatiotemporally associated with spermiation in the rat. *J Androl.* 1999;20:198–213.

Wu H, Reynolds AB, Kanner SB, Vines RR, Parsons JT. Identification and characterization of a novel cytoskeleton-associated pp60^{src} substrate. *Mol Cell Biol.* 1991;11:5113–5124.

Wu H, Parsons JT. Cortactin, an 80/85-kilodalton pp60^{src} substrate, is a filamentous actin-binding protein enriched in the cell cortex. *J Cell Biol.* 1993;120:1417–1426.

Yamamoto T, Taya S, Kaibuchi K. Ras-induced transformation and signaling pathway. *J Biochem.* 1999;126:799–803.

Zhao Z, Tan Z, Diltz CD, You M, Fischer EH. Activation of mitogen-activated protein (MAP) kinase pathway by pervanadate, a potent inhibitor of tyrosine phosphatases. *J Biol Chem.* 1996;271:22251–22255.